

DISCLAIMER

This contractor document was prepared for the U.S. Department of Energy (DOE), but has not undergone programmatic, policy, or publication review, and is provided for information only. The document provides preliminary information that may change based on new information to be used specifically for Total System Performance Assessment analyses. The document is a preliminary lower-level contractor document and is not intended for publication or wide distribution.

Although this document has undergone technical reviews at the contractor organization, it has not undergone a DOE policy review. Therefore, the views and options of authors expressed may not state or reflect those of the DOE. However, in the interest of the rapid transfer of information, we are providing this document for your information per your request.

NMSSD7

**OFFICE OF CIVILIAN RADIOACTIVE WASTE MANAGEMENT
ANALYSIS/MODEL COVER SHEET**

1. QA: QA

Page: 1 of 42

Complete Only Applicable Items

2. Analysis Check all that apply

Type of Analysis	<input type="checkbox"/> Engineering
	<input checked="" type="checkbox"/> Performance Assessment
	<input checked="" type="checkbox"/> Scientific
Intended Use of Analysis	<input type="checkbox"/> Input to Calculation
	<input type="checkbox"/> Input to another Analysis or Model
	<input checked="" type="checkbox"/> Input to Technical Document
	<input type="checkbox"/> Input to Other Technical Products
Describe use: This AMR provides saturated-zone colloid retardation factor distributions for use in PA other transport studies.	

3. Model Check all that apply

Type of Model	<input checked="" type="checkbox"/> Conceptual Model	<input type="checkbox"/> Abstraction Model
	<input type="checkbox"/> Mathematical Model	<input type="checkbox"/> System Model
	<input type="checkbox"/> Process Model	
Intended Use of Model	<input type="checkbox"/> Input to Calculation	
	<input type="checkbox"/> Input to another Model or Analysis	
	<input checked="" type="checkbox"/> Input to Technical Document	
	<input type="checkbox"/> Input to Other Technical Products	
Describe use: The model provides a representation of the chemical and physical processes governing retardation of colloids and saturated material.		

4. Title:
Saturated Zone Colloid-Facilitated Transport

5. Document Identifier (including Rev. No. and Change No., if applicable):
ANL-NBS-HS-000031, Rev 00

INFORMATION COPY
LAS VEGAS DOCUMENT CONTROL

6. Total Attachments: 0

7. Attachment Numbers - No. of Pages in Each:
N/A

	Printed Name	Signature	Date
8. Originator	Andrew Wolfsberg	<i>Andrew Wolfsberg</i>	5-10-00
	Paul Reimus	<i>Clifford K. Ho for P.R.</i>	5/10/2000
9. Checker	Hans Papenguth	<i>Hans Papenguth</i>	5/10/00
10. Lead/Supervisor	Bill Arnold	<i>Bill W. Arnold</i>	5/10/00
11. Responsible Manager	Clifford K. Ho	<i>Clifford K. Ho</i>	5/10/2000

12. Remarks:
AMR S0035

Per Section 5.5.6 of AP-3.10Q, the responsible manager has determined that the subject AMR is not subject to AP-2.14Q review because the analysis does not affect a discipline or area other than the originating organization, Performance Assessment (PA). The downstream user of the information resulting from this AMR is PA, which is also the originating organization of this work. PA lead Bill Arnold and PA customer Stephanie Kuzio have worked with the originators during the development of this AMR. The downstream customers were given the opportunity to provide informal comments on draft copies and to request a formal review if desired. However, it was determined that this analysis does not directly affect other organizations other than the originating organization. Therefore, no formal AP-2.14Q reviews were requested or determined to be necessary.

**OFFICE OF CIVILIAN RADIOACTIVE WASTE MANAGEMENT
ANALYSIS/MODEL REVISION RECORD**

Complete Only Applicable Items

1. Page: 2 of 42

2. Analysis or Model Title:

Saturated Zone Colloid-Facilitated Transport

3. Document Identifier (including Rev. No. and Change No., if applicable):

ANL-NBS-HS-000031, Rev 00

4. Revision/Change No.

5. Description of Revision/Change

00

Initial issue

CONTENTS

	Page
1. PURPOSE.....	7
2. QUALITY ASSURANCE.....	8
3. COMPUTER SOFTWARE AND MODEL USAGE.....	9
4. INPUTS.....	10
4.1 DATA AND PARAMETERS	10
4.2 CRITERIA	11
5. ASSUMPTIONS.....	12
6. ANALYSIS/MODEL.....	15
6.1 COLLOID TRANSPORT IN FRACTURED TUFF.....	15
6.1.1 Background.....	15
6.1.2 Interpretations of Microsphere Responses in Tracer Tests.....	17
6.1.3 Development of Cumulative Probability Density Functions.....	21
6.1.4 Validity of the Local Equilibrium Assumption in Estimating Retardation for Saturated Fractured Tuff.....	24
6.1.5 Uncertainty in Assumptions.....	26
6.1.6 Model Summary: Fractured Tuff Colloid Retardation Factors.....	27
6.1.7 Model Validation Summary: Fractured Tuff Colloid Transport.....	27
6.2 COLLOID TRANSPORT IN ALLUVIAL MATERIAL.....	28
6.2.1 Background.....	28
6.2.2 Parameters for Calculation of Retardation Factors.....	28
6.2.3 Calculation of Retardation Factor Distribution.....	31
6.2.4 Validity of the Local Equilibrium Assumption in Estimating Retardation for Saturated Alluvium.....	33
6.2.5 Uncertainty in Assumptions.....	34
6.2.6 Conceptual Model Summary: Alluvial Colloid Retardation Factors.....	36
6.2.7 Model Summary: Alluvial Colloid Retardation Factors.....	37
6.2.8 Model Validation Summary: Alluvial Colloid Transport.....	37
7. CONCLUSIONS.....	38
8. INPUTS AND REFERENCES.....	40
8.1 DOCUMENTS CITED.....	40
8.2 CODES, STANDARDS, REGULATIONS, AND PROCEDURES.....	41
8.3 SOFTWARE.....	41
8.4 SOURCE DATA, LISTED BY DATA TRACKING NUMBER	41

FIGURES

	Page
1. Composite Fit to the 360-nm Diameter Microsphere Response in the Bullfrog Tuff Tracer Test	18
2. Fits to the Microsphere Responses in the Prow Pass Tuff Tracer Test.	20
3. Discrete Cumulative Probability Density Function for Microsphere Filtration Rate Constants in the C-Wells Tracer Tests.....	22
4. Discrete Cumulative Probability Density Function for Microsphere Detachment Rate Constants in the C-Wells Tracer Tests.....	22
5. Discrete Cumulative Probability Density Function for Microsphere Retardation Factors in the C-Wells Tracer Tests	23
6. Damkohler Number Distributions for Attachment and Detachment Kinetic Rates (Table 6) for Fractured Tuff.....	26
7. Schematic of GoldSim Model of Equations 4-6 for Alluvial Colloid Retardation Factors. 32	
8. Retardation Factor Distribution for Five Simulations	33
9. Damkohler Number Distributions for Attachment and Detachment Kinetic Rates for Alluvium	34
10. Comparing GoldSim Simulations of Retardation Factors for Four Different Grain-Size Diameter Distributions.....	36

TABLES

	Page
1. Input Data Sources	10
2. Assumptions.....	12
3. Summary of C-Wells Tracer Tests Involving Microspheres	16
4. Filtration and Detachment Rate Constants for the Microspheres in each Subpathway of the Bullfrog Tuff Tracer Test	19
5. Filtration and Detachment Rate Constants for the Microspheres in the Prow Pass Tuff Tracer Test	20
6. Values Used for Cumulative Probability Density Functions Shown in Figures 3 through 5	23
7. Parameters for Retardation Factor Calculations and Uncertainty Range Distributions	31

ACRONYMS AND ABBREVIATIONS

AMR	Analysis and Modeling Report
CML	Carboxylate-modified latex
CRWMS M&O	Civilian Radioactive Waste Management System Management and Operating Contractor
DTN	Data tracking number
OCRWM	Office of Civilian Radioactive Waste Management
PA	Performance Assessment
PMR	Process Model Report
QA	Quality assurance
QARD	Quality Assurance Requirements and Description
RTA	Reactive Transport Application
SAN	Software Activity Number
SR	Site recommendation
STN	Software Tracking Number
SZ	Saturated zone
TSPA	Total Systems Performance Assessment
UZ	Unsaturated zone
VA	Viability Assessment
YMP	Yucca Mountain Site Characterization Project

1. PURPOSE

The purpose of the Saturated Zone Colloid-Facilitated Transport Analysis and Modeling Report (AMR), as outlined in its Work Direction and Planning Document (CRWMS M&O 1999a), is to provide retardation factors for colloids with irreversibly-attached radionuclides, such as plutonium, in the saturated zone (SZ) between their point of entrance from the unsaturated zone (UZ) and downgradient compliance points. Although it is not exclusive to any particular radionuclide release scenario, this AMR especially addresses those scenarios pertaining to evidence from waste degradation experiments, which indicate that plutonium and perhaps other radionuclides may be irreversibly attached to colloids.

This report establishes the requirements and elements of the design of a methodology for calculating colloid transport in the saturated zone at Yucca Mountain. In previous Total Systems Performance Assessment (TSPA) analyses, radionuclide-bearing colloids were assumed to be unretarded in their migration. Field experiments in fractured tuff at Yucca Mountain and in porous media at other sites indicate that colloids may, in fact, experience retardation relative to the mean pore-water velocity, suggesting that contaminants associated with colloids should also experience some retardation. Therefore, this analysis incorporates field data where available and a theoretical framework when site-specific data are not available for estimating plausible ranges of retardation factors in both saturated fractured tuff and saturated alluvium. The distribution of retardation factors for tuff and alluvium are developed in a form consistent with the Performance Assessment (PA) analysis framework for simulating radionuclide transport in the saturated zone.

To improve on the work performed so far for the saturated-zone flow and transport modeling, concerted effort has been made in quantifying colloid retardation factors in both fractured tuff and alluvium. The fractured tuff analysis used recent data and interpretation from the C-wells reactive tracer testing complex in the saturated zone of Yucca Mountain. As no data regarding colloid transport have been developed by the Yucca Mountain Site Characterization Project (YMP) for the alluvial system, a theoretical analysis based on studies performed in other alluvial systems is developed. The parameters derived in this AMR are developed in a manner consistent with the PA methodology and can be readily integrated into that analysis.

The work activities in this AMR are governed by the Work Direction and Planning Document (CRWMS M&O 1999a) for abstraction of colloid facilitated plutonium transport. The purpose and scope of the activity is to abstract colloid-facilitated transport parameters for use in TSPA analyses. While the general scope of this activity has remained the same, specific tasks have been modified to better address the evolving needs of TSPA. The codes RTA V1.1 (Software Tracking Number (STN): 10032-1.1-00) and GoldSim V6.03 (STN: 10296-6.03-00) were used in this AMR rather than FEHM, which was originally planned (CRWMS M&O 1999a). RTA was developed with a specific goal of interpreting colloid transport parameters in fractured tuff at Yucca Mountain. GoldSim, which is a standard code used in the Yucca Mountain PA analyses, was used for analysis of retardation factors in alluvium because large ranges in uncertainty had to be addressed due to the lack of site-specific data for this process. This approach replaced the 1-D simulations that were originally planned (CRWMS M&O 1999a).

2. QUALITY ASSURANCE

The activities documented in this Analysis/Model Report (AMR) were evaluated in accordance with QAP-2-0, *Conduct of Activities*, and were determined to be subject to the requirements of the U.S. DOE Office of Civilian Radioactive Waste Management (OCRWM) *Quality Assurance Requirements and Description* (QARD) (DOE 2000). This evaluation is entitled *Conduct of Performance Assessment* (CRWMS M&O 1999b). This AMR has been prepared in accordance with procedure AP-3.10Q, *Analyses and Models*.

3. COMPUTER SOFTWARE AND MODEL USAGE

The computer software codes used in this AMR are as follows.

1. *Software:* Reactive Transport Application (RTA), V1.1, (STN: 10032-1.1-00)

Used for: Analysis of colloid retardation in the C-wells tracer test

The software was obtained from Configuration Management, is appropriate for the application, and was used only within the range of validation in accordance with AP-SI.1Q.

2. *Software:* GoldSim, V6.03 (STN: 10296-6.03-00)

Used For: Theoretical model of colloid retardation factors in alluvial material

The software is appropriate for the application and was used only within a range for which it was developed. The input and output files for these analyses are being submitted to the YMP database for archival. The software is currently unqualified and is being controlled per Section 5.11 of AP-SI.1Q Software Management.

3. *Software:* Microsoft Excel, 97 SR-1

Used for: Plotting graphs

Only built-in standard functions in this commercial software were used. No software routines or macros were used to prepare this report. No numerical models were used in report preparation.

4. INPUTS

This document may be affected by technical product input information that requires confirmation. Any changes to the document that may occur as a result of completing the confirmation activities will be reflected in subsequent revisions. The status of the input information quality may be confirmed by review of the Document Input Reference System database.

4.1 DATA AND PARAMETERS

Table 1. Input Data Sources

Data Description	Data Sources	Location in this Document
Fractured Tuff Analysis		
Bullfrog Tuff tracer test data	DTN: LA0002PR831231.001	Fig. 1
Prow Pass reactive tracer test field data	DTN: LAPR831231AQ99.001	Fig. 2
Interpretations of Bullfrog Tuff tracer test data	DTN: LA9909PR831231.003	Fig. 1, Table 4, Table 6, Fig. 3, Fig. 4, Fig. 5
Bullfrog test production rate/recirculation rate	DTN: GS981008312314.002 GS981008312314.003 GS970708312314.007	Table 3
Prow Pass test production rate/recirculation rate	DTN: GS990408312315.002	Table 3
Bullfrog solute mean residence time	DTN: LA9909PR831231.003	Table 3
Prow Pass solute mean residence time	DTN: LA9909PR831231.005	Table 3, Fig. 3, Fig. 4, Fig. 5

Table 1. Input Data Sources (Continued)

Data Description	Data Sources	Location in this Document
Specific discharge distribution and porosity distribution in tuff	DTN: SN0004T0571599.004	Fig. 6
Alluvial Material Analysis		
Data Description	Data Sources	Location in this Document
Porosity distribution in alluvium	DTN: SN0004T0571599.004	Section 6.1.4, Table 7, Figs. 6-10
Specific discharge (Flux) (q) (m/yr) in alluvium	DTN: SN0004T0501600.004	Table 7, Figs. 7-10
Alluvial bulk density is 1.27 g/cm ³	DTN: LA0002JC831341.001	Section 6.2.2
Colloid size distribution	DTN: LL991109751021.094	Table 7, Figs. 7-10, Section 6.1.5

4.2 CRITERIA

No system description documentation (SDD) criteria are available at this time. This AMR complies with the DOE interim guidance (Dyer 1999). Subparts of the interim guidance that apply to this analysis or modeling activity are those pertaining to the characterization of the Yucca Mountain site (Subpart B, Section 15), the compilation of information regarding hydrogeology and geochemistry of the site in support of the License Application (Subpart B, Section 21(c)(1)(ii)), and the definition of hydrogeologic parameters and conceptual models used in performance assessment (Subpart E, Section 114(a)).

5. ASSUMPTIONS

The underlying assumptions of the radionuclide transport model are outlined in this section as the first step toward developing the conceptual, mathematical, and computational models needed in PA calculations.

Table 2. Assumptions

Location In this AMR	Category	Assumption	Basis
Sections 6.1.1 and 6.1.2.	Colloid location	Flow only in fractures. Colloids have diffusion coefficients at least three orders of magnitude smaller than solutes, and because of this and their large size, they will be not be able to negotiate significant matrix tortuosity.	Colloid-size range is larger than mean pore size of fractured volcanic tuffs.
Sections 6.1.1 and 6.1.2.	Flow domain	Constant aperture and flow rate throughout fracture model domain.	Philosophy was to use models that were only as sophisticated as knowledge of the system could support. Model complexity was introduced incrementally and only as necessary to match the field data. An example of additional complexity was the introduction of multiple flow pathways to match the Bullfrog test field data.
Sections 6.1.1	Colloid transport	Colloids experience the same mean residence time and hydrodynamic dispersivity in fractures as solutes.	Standard assumption in colloid transport modeling (e.g., Harvey and Garabedian, 1991).
Sections 6.1.1, 6.1.6, and Fig. 2.	Filtration parameters	Colloid attachment and detachment described by first-order rate expressions (fracture only).	RTA model simulates attachment and detachment with first-order kinetics and matches field observations. Data do not warrant more complex forms of the equation.
Section 6.	Applicability of microsphere studies	Carboxylate-modified-latex microspheres are suitable analogs for natural colloids.	Engineered microspheres were selected to optimize transport. Therefore, using them as an analog for natural colloids should be conservative.
Sections 6.1.4 and 6.2.4.	Local equilibrium assumption	Filtration and detachment rates of colloids to/from immobile surfaces is fast enough, relative to the porewater velocity, that the process can be modeled with an equilibrium formulation.	Damkohler number analyses conducted in Section 6.1 and 6.2 of this AMR, which show that the rates are sufficiently fast relative to water velocities that there is no difference between kinetic and equilibrium formulations, or that, at worst, the kinetic formulation will be conservative.
Section 6.1.3.	Development of probability density function for colloid retardation factor	Results from Prow Pass Tuff and Bullfrog Tuff tracer tests are equally weighted.	Radionuclides will encounter the saturated zone in volcanic units beneath the repository. Both the Prow Pass and Bullfrog Tuffs are present at the water table beneath the repository.

Table 2. Assumptions (Continued)

Location in this AMR	Category	Assumption	Basis
Section 6.1.3.	Development of probability density function for colloid retardation factor	The two pathways identified in the Bullfrog Tuff analysis are equally weighted.	Differences in observed mass distribution between the two flow paths were more likely due to density effects in the borehole rather than natural phenomena.
Section 6.1.3.	Development of probability density function for colloid retardation factor	Within a given pathway in the Bullfrog Tuff, the probabilities of colloids having transport parameters associated with each subpathway is assumed to be proportional to the mass fractions of colloids associated with those subpathways.	The splitting of colloid mass into subpathways was necessary to capture the complexity of the colloid response within each pathway (Reimus et al. 1999)
Section 6.1.3.	Development of probability density function for colloid retardation factor	The two microsphere responses in the Prow Pass test are equally weighted.	Only one pathway is evaluated. The two different microsphere types are equally likely analogs for natural colloid transport.
Section 6.	Pu-colloid form	For Pu-bearing colloids reaching the SZ, the Pu is irreversibly attached to the colloids. Although the retardation factors computed in this AMR are applicable to ALL colloids. The assumption only relates to the reason that this AMR does not address Pu-colloid reactions.	Indications from the <i>Colloid-Associated Radionuclide Concentration Limits</i> AMR (CRWMS M&O 2000a, Sec. 6.2) are that the plutonium is embedded within the released colloids as well as reversibly sorbed onto them.
Sections 6.2.2 and 6.2.3.	Colloid density	Assumed to be equivalent to montmorillonite.	Density of plutonium-bearing colloids from waste form has not been measured, but has been identified as clay.
Table 7, Fig. 7, Fig. 8, Fig. 9, Fig. 10.	Alluvial grain size distribution	Ranges from 0.02 to 0.11 cm (fine, medium, and coarse grain sands). [Size correlation to sand type based on the United States Department of Agriculture size fractions (Marshall et al. 1996; Fig. 1.2, p. 4)]	We are not aware of any completed analyses of grain size distributions in the Yucca Mountain valley fill alluvium. Therefore, we use analyses from Yucca Flat as a surrogate (knowing that YMP will soon have material analyses that can be used to supercede these). Bechtel (1998a) reported on the weight fraction of sand, silt, and clay in two alluvial boreholes in Yucca Flat. In the samples collected, sand was the dominant material with a weight fraction greater than 80%. Thus, we conservatively assume that the YM valley-fill alluvium system is sand. Marshall et al. (1996, Fig. 1.2, p. 4) show that the grain sizes represented by fine, medium, and coarse sands range between .02 and .11 cm.

Additional ranges used in uncertainty analysis in Section 6.2.5.			<p>Further review of a Bechtel data report (Bechtel 1998b) indicates that their grain size distribution for sand ranges from 0.005 to 0.2 cm. Therefore, sensitivity analysis in this AMR compares this slightly larger range to the range used for the PA calculations.</p> <p>It should be noted that horizons with grains much larger than a coarse sand are likely to have their interstitial spaces filled by finer material, and horizons with grain sizes much smaller (e.g., clays) are unlikely to transmit much water.</p>
Sections 6.2.1, 6.2.2, 6.2.3, and 6.2.8.	Colloid filtration in alluvium	Attachment rate can be predicted with kinetic filtration theory.	In the absence of YMP data, the Cape Cod site is used as an analog (Harvey and Garabedian 1991, Table I, p. 179). Kinetic filtration theory was used to predict colloid attachment to immobile grains in that study (Harvey and Garabedian 1991, Eqs. 1, 2, 6, and p. 184)
Sections 6.2.2 and 6.2.3, Table 7, Fig. 7, Fig. 8, Fig. 9, Fig. 10	Colloid filtration in alluvium	Distribution range for Alpha parameter (collision efficiency factor) in kinetic filtration theory, is between 0.005 and 0.025.	This is the range of collision efficiency factors found by Harvey and Garabedian (1991, p. 181, Table II) for bacterial and microsphere colloids in the Cape Cod sand aquifer. This is probably a conservative range since collision efficiency factors may be higher in Yucca Mountain alluvium if the material is less well-sorted than the uniform sand at Cape Cod.
Sections 6.2.2 and 6.2.3.	Colloid filtration in alluvium	Detachment rate range should cover the range of detachment rates of colloids and microspheres from fracture surfaces.	Although detachment has not been measured for Yucca Mountain alluvium, the process of detachment from alluvial grains may be similar to the process of detachment from fracture surfaces.
Sections 6.2.2 and 6.2.3, Table 7.	Colloid filtration in alluvium	Detachment rate range should also cover the range measured for microspheres and bacteriophages in the Borden Sand aquifer. This extends the lower range of detachment rates that were estimated for for fracture surfaces down from 1E-4 to 1E-5.	<p>Detachment rates of microspheres and bacteriophages were measured in a limited experiment at the Borden Sand aquifer (Bales et al. 1997, Table 3, parameter k2)</p> <p>In the absence of Yucca Mountain specific data, the range of detachment rates of colloids from porous media surfaces should include the values from the Borden aquifer.</p>
Section 6.2.2 and 6.2.3	Colloid filtration in alluvium	Water temperature is 25° Celsius	Sass et al. (1988) [DTN: GS950408318523.001] measured surface water temperatures to be about 20 degrees Celsius and a geothermal gradient of about 25 degrees per 1000 meters. Alluvial flow and transport are considered to occur only in the shallow part of the aquifer, so a temperature of 25 degrees represents the temperature at about 200 meters depth.

6. ANALYSIS/MODEL

The primary cause of colloid retardation is attachment and detachment from immobile surfaces. This analysis demonstrates the development of parameters necessary to estimate attachment and detachment of colloids and, hence, retardation in both fractured tuff and porous alluvium. Field data are used for the analysis of colloid retardation in fractured tuff. Due to the lack of any field data for colloid transport in alluvial material, a theoretical analysis developed at another site is implemented in this analysis.

6.1 COLLOID TRANSPORT IN FRACTURED TUFF

This report considers the migration of plutonium-colloids where, based on CRWMS M&O 2000a, Sec. 6.2) the plutonium is assumed to be irreversibly attached to colloids (Table 2).

6.1.1 Background

The colloid transport parameters developed for this AMR were derived from field tracer tests conducted in fractured volcanic tuffs at the C-wells, UE25-C#1, #2, and #3 (Reimus et al. 1999). The colloid tracers used at the C-wells were fluorescent carboxylate-modified latex (CML) polystyrene microspheres (Interfacial Dynamics Corp., Portland, Oregon). Table 3 summarizes the colloid tracer tests and microspheres used at the C-wells. Carboxylate-modified latex (CML) microspheres were chosen as field tracers because of the following: (1) they can be tagged with different fluorescent dyes that allow them to be quantified even at concentrations several orders of magnitude below background colloid concentrations; (2) they have a negative surface charge similar to rock surfaces and presumably natural colloids; and (3) they are more hydrophilic than other microspheres, which makes them more resistant to attachment and flocculation, even at higher ionic strengths (hence, making them good "conservative" colloid tracers). The pK_a of carboxylic acid is around 5, and the C-wells groundwater pH was 7 to 8; therefore, the microspheres should have been negatively charged in the field tracer tests. Also, because of their hydrophilic surfaces, the CML microspheres are relatively stable even at ionic strengths approaching 1 molar (in monovalent cations), which is advantageous when injecting them with ionic solute tracers. CML microspheres behaved more conservatively (less attachment) than silica microspheres and non-modified carboxylated latex microspheres (hydrophobic surfaces) in previous laboratory experiments (Reimus 1995). The use of conservative colloid tracers was expected to result in conservative filtration parameter estimates, which in turn should result in conservative predictions of large-scale colloid transport.

In the C-wells field tracer tests, the microsphere responses were interpreted by comparing them to the responses of nonsorbing solute tracers that were injected either simultaneously with or just after the microspheres. The responses of the nonsorbing solutes were fitted using a semi-analytical, dual-porosity mass-transport computer model, Reactive Transport Application (RTA V1.1), to obtain estimates of the fractional mass participation, tracer mean-residence times, dispersivities, and matrix-diffusion mass-transfer coefficients in the flow system(s). The fractional mass participation is simply the fraction of the injected tracer mass accounting for the observed response or for a portion of the observed response (e.g., one of two peaks). Fractional mass participation could be physically caused by (1) a finite volumetric flow rate into the matrix

that acts as a sink for tracers because its velocity is much too low for tracers to appear at the production well; (2) stagnation point(s) resulting from the weak recirculation in the tests, or

Table 3. Summary of C-Wells Tracer Tests Involving Microspheres

Test Parameter	Bullfrog Tuff	Prow Pass Tuff
Injection/Production Wells	UE25-c#2 / c#3	UE25-c#3 / c#2
Interval, m below surface ⁽¹⁾	800-900	630-705
Production Flow Rate, L/min	568	19.5
Fraction Recirculated ⁽²⁾	0.033	0.3
Mean Solute Residence Time ⁽³⁾ , hrs	37, 995	1230
Nonsorbing Solutes ⁽⁴⁾	Br ⁻ , PFBA ⁻	Br ⁻ , Cl ⁻ , PFBA ⁻
		280 / orange ⁽⁵⁾
Microsphere Diameter, nm / Dye	360 / yellow	280 / yellow ⁽⁵⁾ 640 / blue

DTNs: Bullfrog test flow rate: GS981008312314.003, GS97078312314.007, GS981008312314.002; Prow Pass test flow rate: GS990408312315.002; Bullfrog test mean residence time: LA9909PR831231.003; Prow Pass test mean residence time: LA9909PR831231.005

- NOTES:
- (1) Intervals are approximate because packer locations were different in each well. Water table is ~400 m below surface.
 - (2) Fraction of produced water recirculated into the injection well.
 - (3) Two mean residence times are listed for the Bullfrog Tuff, one for each of the two tracer peaks.
 - (4) PFBA⁻ is pentafluorobenzoate.
 - (5) The 280-nm yellow and orange microspheres were the same spheres, but they were tagged with different fluorescent dyes because they were injected at different times.

(3) loss of tracer due to a portion of the relatively dense injection solution "sinking" out of the zone of influence of pumping. The matrix-diffusion mass transfer coefficient is a lumped parameter (porosity times square root of matrix diffusion coefficient divided by average fracture half-aperture, time^{-1/2}) that describes the diffusive mass transfer rate of solutes between fractures and matrix.

It was assumed that the fractional mass participation, the mean-residence times, and dispersivities obtained for the solutes also applied to the microspheres (e.g., Harvey and Garabedian, 1991). However, because of their large size and small diffusivities compared to the solutes (approximately 3 orders-of-magnitude smaller), it was assumed that there was no matrix diffusion of microspheres (matrix-diffusion coefficient was set equal to zero). The advection-dispersion equation with appropriate terms for a single reversible first-order reaction to account for mass transfer between mobile water and immobile surfaces (filtration and detachment) was used to model microsphere transport:

$$\frac{\partial C}{\partial t} + V \frac{\partial C}{\partial x} - D \frac{\partial^2 C}{\partial x^2} + k_{\text{fil}} C - k_{\text{res}} S = 0 \quad (\text{Eq. 1})$$

$$\frac{1}{b} \frac{\partial S}{\partial t} - k_{\text{fil}} C + k_{\text{res}} S = 0 \quad (\text{Eq. 2})$$

where

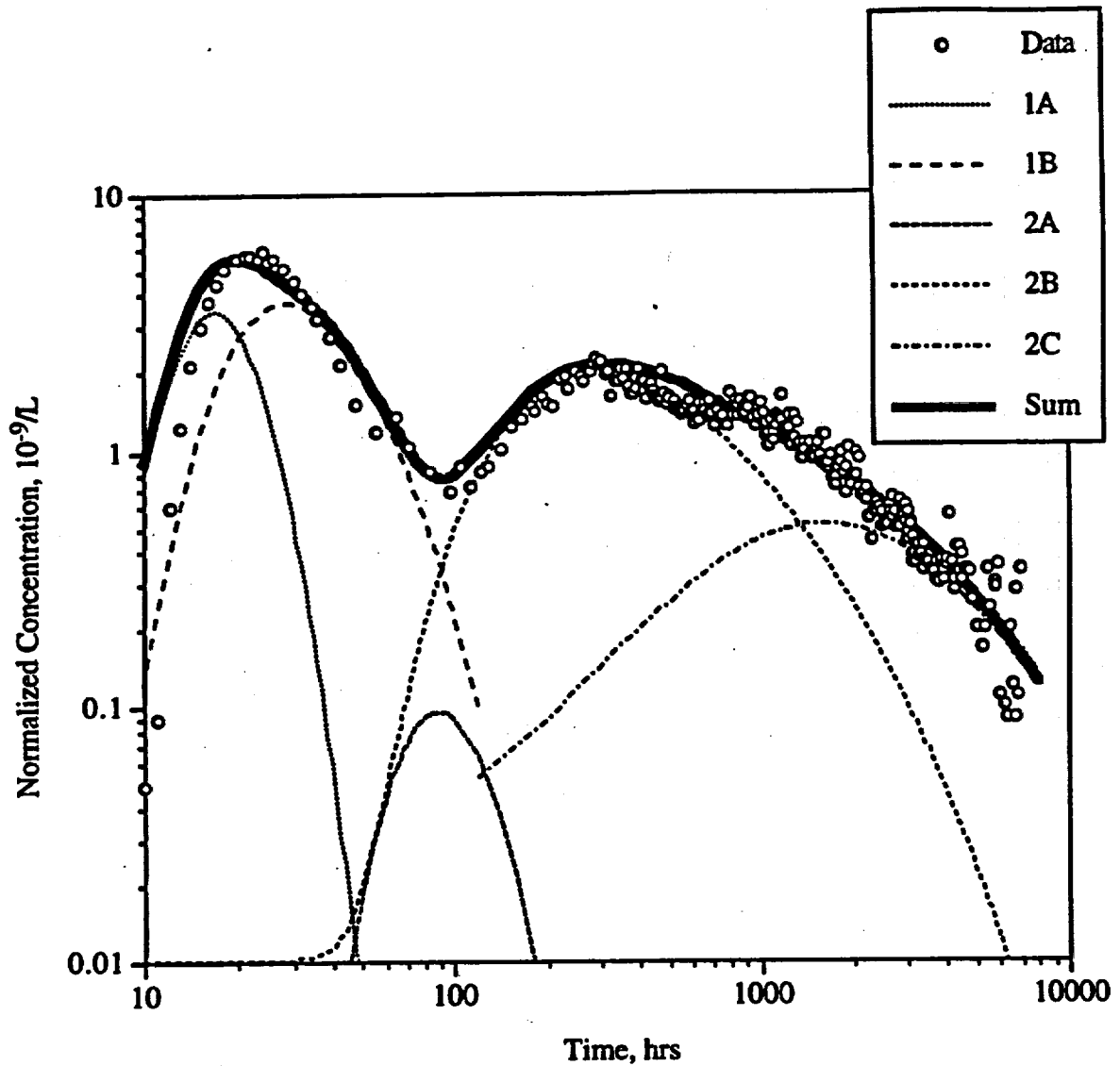
- C = colloid concentration in solution, no./L
- S = colloid concentration on fracture surfaces, no./cm²
- V = flow velocity in fractures, cm/sec
- D = dispersion coefficient, cm²/sec
- k_{filt} = filtration rate constant (1/sec) = λV, where λ = filtration coefficient (1/cm)
- k_{res} = detachment rate constant, 1/cm-sec
- x, t = independent variables for distance and time, respectively.
- b = fracture half aperture (cm).

The values for V and D in Equations 1 and 2 were obtained from the interpretation of the nonsorbing solute tracer responses; therefore, the filtration and detachment rate constants were the only parameters adjusted to match the microsphere responses. Details of the interpretation procedure for both the Bullfrog Tuff and Prow Pass Tuff tracer tests are provided in Reimus et al. (1999).

6.1.2 Interpretations of Microsphere Responses in Tracer Tests

The interpretation of the Bullfrog Tuff tracer test was complicated by the fact that the breakthrough curves of all tracers were bimodal. This problem was addressed by treating each "peak" as being the result of a separate set of flow pathways, each with its own set of transport parameters, which, when added together, resulted in the observed composite response. The term "pathway" is henceforth used in this AMR to refer to such sets of flow pathways (loosely defined as pathways that, when lumped together, result in a tracer response that can be described using a single set of parameters in the advection-dispersion equation). Using the relatively simple model represented by Equations 1 and 2, it was not possible to match the 360-nm microsphere response with a single set of filtration parameters for either peak. Instead, the microsphere mass in each pathway was divided into subsets that were assumed to experience different detachment rates due to both physical and chemical heterogeneities in the system. These subsets of mass are referred to as "subpathways" because they represent a fraction of the total transport within a given "pathway." All of the microsphere mass in each of the two primary pathways was assumed to experience the same forward filtration rate (defined as the "forward" component of reversible filtration).

Figure 1 shows the resulting composite fit to the microsphere response in the Bullfrog Tuff test along with the predicted contributing responses of each "subpathway." The filtration and detachment rate constants associated with the subpathways are listed in Table 4. Note that the detachment rate constants for subpathways 1A and 2A are the maximum values that can be used without degrading the overall fit to the response at late times. That is, if larger detachment rate constants were used, the tail of the predicted response would be raised higher than the data. However, the overall fit to the data would be just as good if k_{res} in subpathways 1A and 2A were set equal to zero (i.e., irreversible filtration); hence, this interpretive procedure can only establish maximum detachment rate constants. These maximum values should yield the most conservative (fastest) colloid transport predictions.



DTNs: LA0002PR831231.001 for data, LA9909PR831231.003 for model input data.

NOTE: Normalized concentration is 10^9 times particles/L divided by the total number of particles injected.

Figure 1. Composite Fit to the 360-nm Diameter Microsphere Response in the Bullfrog Tuff Tracer Test

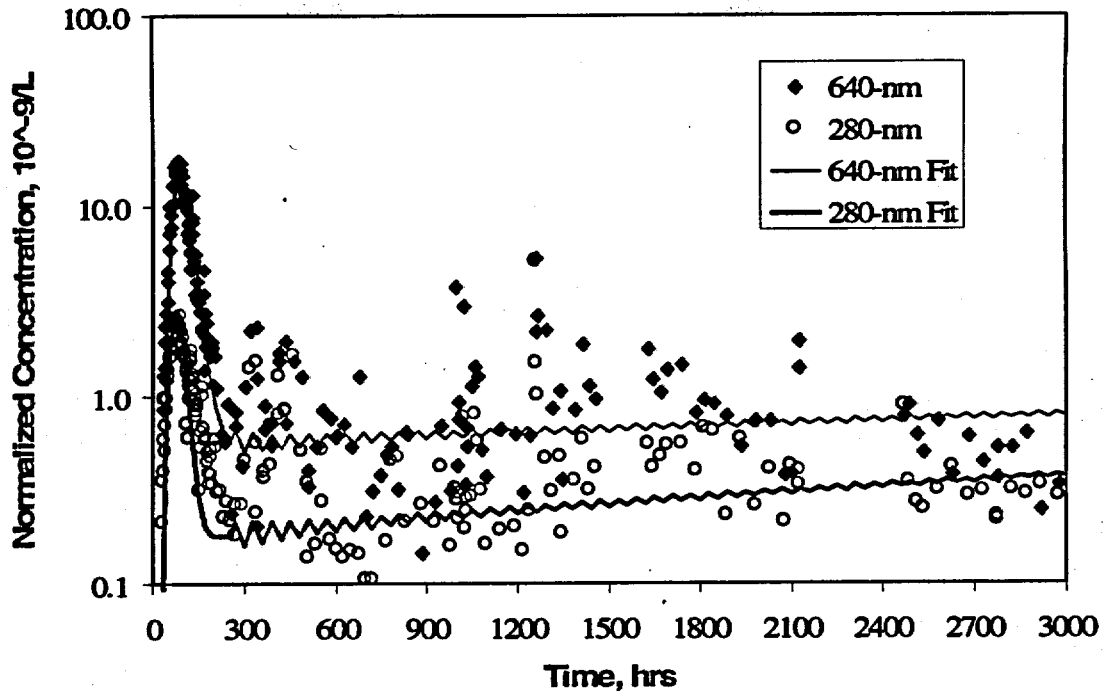
Table 4. Filtration and Detachment Rate Constants for the Microspheres in each Subpathway of the Bullfrog Tuff Tracer Test

Parameter	Path 1A	Path 1B	Path 2A	Path 2B	Path 2C
f, mass fraction	0.115	0.005	0.423	0.067	0.1
k_{fit} , 1/hr	0.2	0.2	0.04	0.04	0.04
$\lambda^{(1)}$, 1/cm	0.00247	0.00247	0.0133	0.0133	0.0133
$bk_{res}^{(2)}$, 1/hr	0.00025 ⁽³⁾	3.33	0.000404 ⁽³⁾	0.4	0.008

DTNs: LA9909PR831231.003 (for mass fractions and detachment rate constants for paths 1B, 2B, and 2C).

- NOTES: ⁽¹⁾ λ = filtration coefficient, calculated as k_{fit}/V , where V = average linear velocity determined from mean fluid residence time.
⁽²⁾ b = fracture half aperture, cm. The fitted detachment rate constant is this lumped parameter.
⁽³⁾ Maximum detachment rate constant; cannot distinguish between this value and zero.

The interpretation of the Prow Pass Tuff tracer test was much more straightforward than that for the Bullfrog Tuff test. A single set of filtration parameters could adequately explain the responses of both microspheres. Figure 2 shows the resulting fits to the microsphere responses, and Table 5 lists the filtration parameters corresponding to these fits. Note that the 280-nm yellow microspheres never appeared at the production well. These spheres were injected in the same solution as the solute tracers, which had an ionic-strength solution of ~ 0.4 M due to the high solute masses/concentrations necessary to ensure quantifiable responses at the production well. It is suspected that the spheres quickly attached to fracture surfaces or to each other because of the destabilizing effect of the high ionic strength. The filtration and detachment rate constants reported for these microspheres are the minimum and maximum values, respectively, that result in no predicted response of these colloids. That is, any smaller value of the filtration rate constant or larger value of the detachment rate constant would result in a small predicted response that was not observed. Because the yellow microspheres were injected in such a high ionic-strength solution, they were not considered in the development of cumulative probability density functions for colloid transport parameters (see below). Their inclusion in this analysis would raise the probabilities of high-filtration-rate constants and low-detachment-rate constants, which would raise the probability of high retardation factors. Thus, their omission from the following analysis is considered conservative. The yellow spheres were injected with the solute tracers primarily because this was the only practical way of investigating the effect of solution ionic strength on colloid transport in the field tests.



DTN: LAPR831231AQ99.001 for data. Output data - DTN: LA9912PR831231.006 for model fits.

NOTES: The zig-zag appearance of the fits at late times is the result of minor instabilities in the inversion algorithm in the RTA model. Normalized concentration is 10^9 times particles/L divided by the total number of particles injected.

Figure 2. Fits to the Microsphere Responses in the Prow Pass Tuff Tracer Test

Table 5. Filtration and Detachment Rate Constants for the Microspheres in the Prow Pass Tuff Tracer Test

Parameters	Microspheres		
	640-nm Blue	280-nm Orange	280-nm Yellow
k_{fit} , 1/hr	0.043	0.07	0.2 ⁽¹⁾
λ , 1/cm	0.017	0.028	0.08
$b_{k_{res}}$ ⁽²⁾ , 1/hr	0.000154	0.000251	0.001

Output data - DTN: LA9912PR831231.006

NOTES: ⁽¹⁾ Minimum value that is consistent with the lack of appearance of these spheres at the production well. The actual filtration rate constant could be much higher.
⁽²⁾ Maximum values; cannot distinguish between these values and zero. See also footnote (2) of Table 3.

6.1.3 Development of Cumulative Probability Density Functions

The assumptions associated with the development of cumulative probability density functions for colloid-filtration-rate constants, detachment-rate constants, and effective retardation factors, based on Reimus et al. (1999), are stated in Table 2.

The assumptions effectively divided the two tracer tests into four equally-weighted "trials."

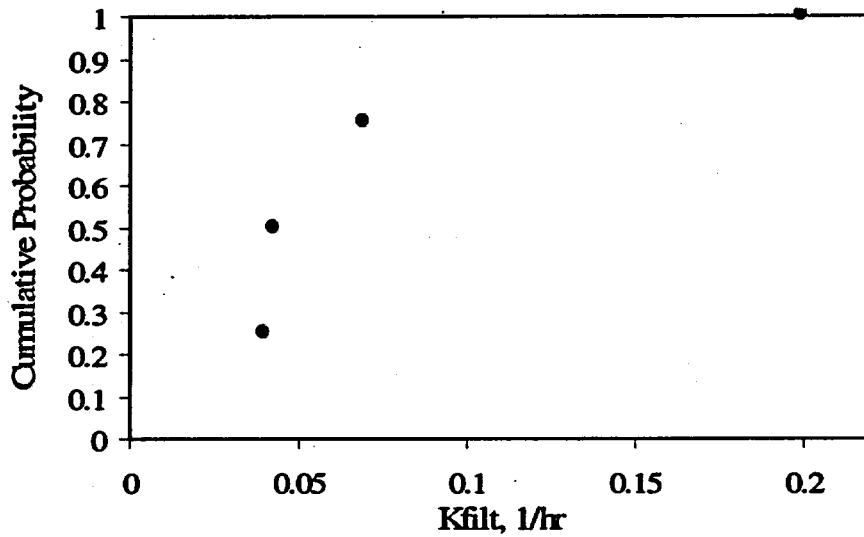
1. The first peak of 360-nm-diameter microspheres in the Bullfrog Tuff test.
2. The second peak of 360-nm-diameter microspheres in the Bullfrog Tuff test.
3. The response of 280-nm-diameter orange microspheres in the Prow Pass test.
4. The response of 640-nm-diameter blue microspheres in the Prow Pass test.

No weights were assigned to the different sizes of microspheres. Thus, the 360-nm spheres used in the Bullfrog Tuff test implicitly were given a higher weighting than the other spheres because they were used in two of the four "trials."

Figures 3 and 4 show the resulting cumulative probability density functions for the microsphere-filtration and detachment-rate constants, respectively. Figure 5 shows the cumulative probability density function for the effective microsphere retardation factor. The points plotted in Figures 3 through 5 are listed in Table 6. The retardation factors, R, in Figure 5 and Table 6 were obtained by applying the following equation in each pathway of each test:

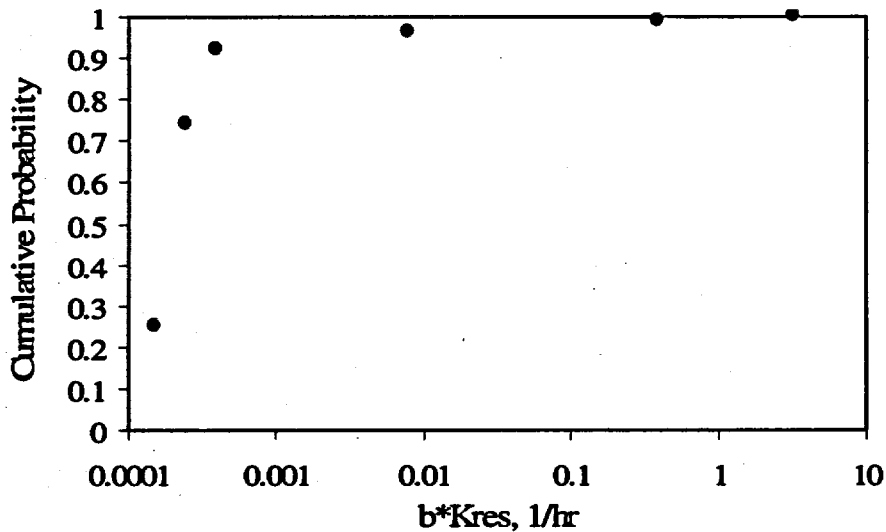
$$R = 1 + \frac{k_{\text{filt}}}{bk_{\text{res}}} \quad (\text{Eq. 3})$$

Thus, the R values were based on actual observations in each pathway; they were *not* developed by independently randomly sampling the two probability density functions in Figures 3 and 4. The former approach effectively captures any *correlations* that may exist between the filtration and detachment rate constants (forward and reverse reactions, respectively), whereas in the latter approach, any correlations will be lost. No analyses were attempted to establish formally such correlations between forward and reverse rates.



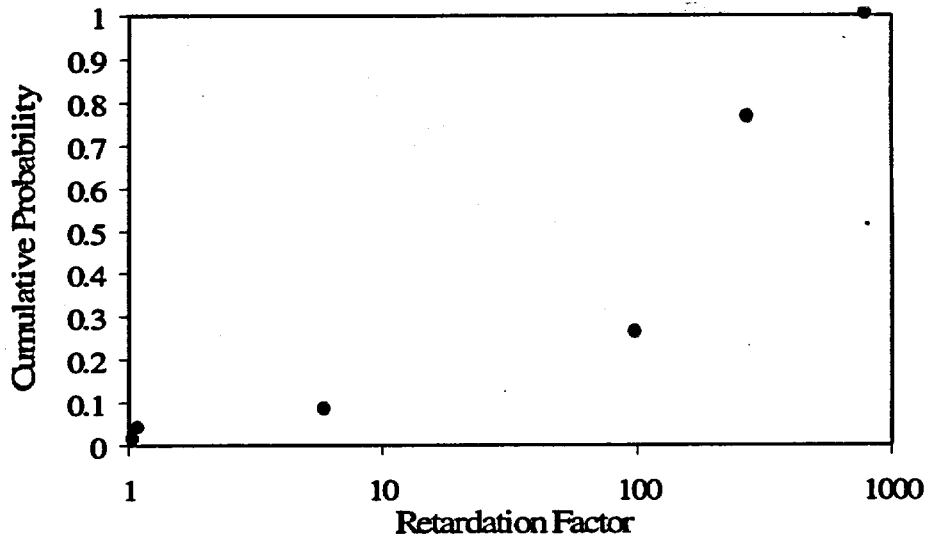
DTNs: LA9909PR831231.003 and LA9909PR831231.005 for model input data.

Figure 3. Discrete Cumulative Probability Density Function for Microsphere Filtration Rate Constants in the C-Wells Tracer Tests



DTN: LA9909PR831231.003 and LA9909PR831231.005 for model input data.

Figure 4. Discrete Cumulative Probability Density Function for Microsphere Detachment Rate Constants in the C-Wells Tracer Tests



DTN: LA9909PR831231.003 and LA9909PR831231.005 for model input data.

Figure 5. Discrete Cumulative Probability Density Function for Microsphere Retardation Factors in the C-Wells Tracer Tests

Table 6. Values Used for Cumulative Probability Density Functions Shown in Figures 3 through 5

Group 1		Group 2		Group 3			
Filtration Only		Detachment Only		Retardation Factors with Coupled Rates Distribution			
k_{fil} , 1/hr	Probability	bk_{res} , 1/hr	Probability	R	k_{fil}	bk_{res}	Probability
0.04	0.25	0.000154	0.25	1.06	0.2	3.33	0.0105
0.043	0.5	0.00025	0.7395	1.1	0.04	0.4	0.039
0.07	0.75	0.000404	0.91875	6	0.04	0.008	0.08125
0.2	1	0.008	0.961	100	0.04	0.0004	0.2605
		0.4	0.9895	280	0.07	0.000251	0.5102
		3.33	1	280	0.043	0.000154	0.7605
				800	0.2	0.00025	1.0

6.1.4 Validity of the Local Equilibrium Assumption in Estimating Retardation for Saturated Fractured Tuff

The length and time scales associated with colloid transport in saturated, fractured tuff will both be significantly larger than those sampled during the forced gradient tests from which these parameters are derived. Therefore, the time scales associated with colloid filtration and detachment in the saturated tuff have been assumed to be small relative to fluid residence times (an assumption necessary for the local equilibrium assumption to be valid). To evaluate the validity of this assumption, a simple analysis can be performed with non-dimensional Damkohler numbers. The Damkohler number is simply the rate constant, k (1/hr), multiplied by a representative residence time, T (hr), $Da=kT$. Bahr and Rubin (1987, p. 440, Equation 12) demonstrate that the mass balance equation describing solute transport can be differentiated into an equilibrium and kinetic component. The smaller the kinetic component, the more accurate are the retardation factors based on the local equilibrium assumption.

For evaluation of colloid behavior, Damkohler numbers, Da_{att} and Da_{det} , can be computed for attachment and detachment of colloids, respectively, using k_{filt} and k_{res} . The magnitude of the kinetic component is inversely proportional to $Da_{att}+Da_{det}$. Thus, the larger the sum of the two Damkohler numbers, the more appropriate the assumption of equilibrium. Bahr and Rubin (1987, p. 450) found that equilibrium was well approximated when the sum of the two Damkohler numbers is greater than 100 and reasonably well estimated when the sum is greater than 10. Valocchi (1985, p. 813, Figure 2) had a similar result, although he only used the reverse rate to compute a Damkohler number similar to Da_{det} in this analysis. Bahr and Rubin (1987) point out that the kinetic term can only be completely separated when the sum of the two Damkohler numbers is used.

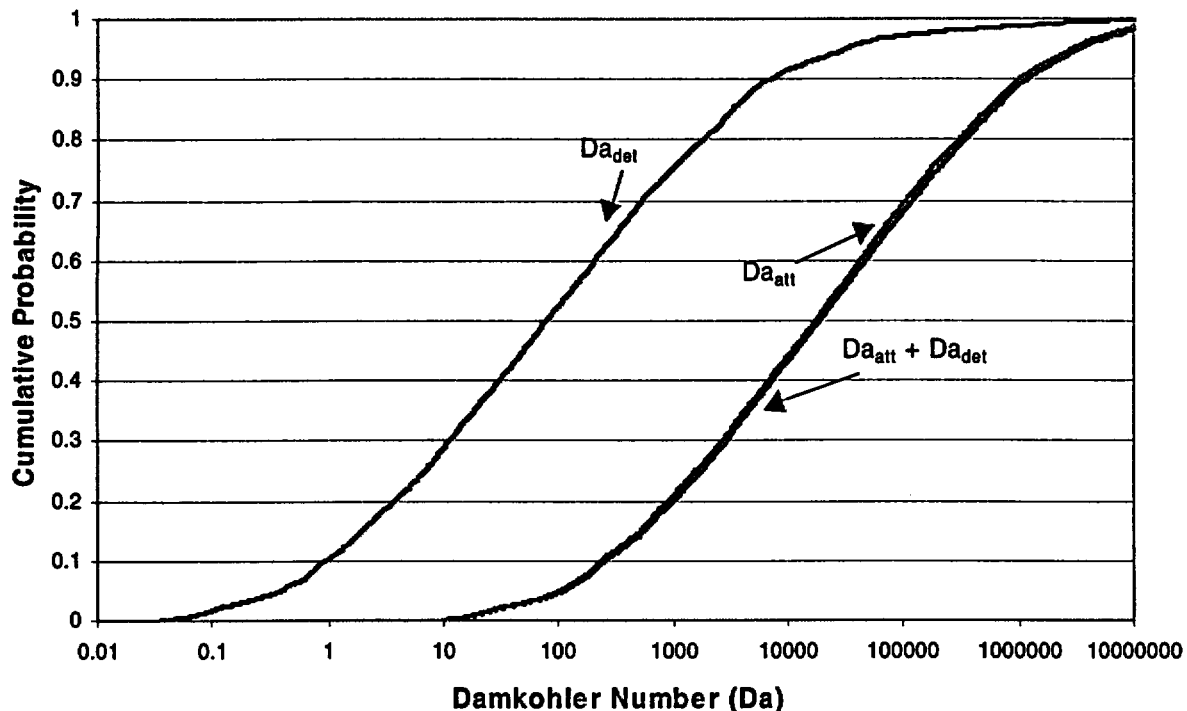
To compute the residence time, T , the length (L), specific discharge (q), and porosity (θ) are needed ($T=L/\theta q$), where porosity is the fracture volume fraction of the domain. A representative length scale, L , for the Yucca Mountain saturated volcanic tuffs is 16,000 meters, but specific discharge and porosity are variable parameters drawn from distributions. The attachment and detachment rates are also drawn from a distribution (Table 6, group 3). Therefore, a GoldSim V6.03 (STN: 10032-1.1-00) model is used to compute cumulative distributions for Da_{att} , Da_{det} , and the sum of the two for this evaluation of the validity of the local equilibrium assumption in estimating retardation factors. The porosity ranges between 0.00001 and 0.1 with a log-uniform distribution, and the specific discharge is characterized with a discrete distribution spanning low, medium, and high rates (0.06 m/yr 24% of the time, 0.6 m/yr 52%, and 6 m/yr 24%) (CRWMS M&O 2000b, DTN SN0004T0571599.004). The low end of the porosity range is well below the porosity estimates from the C-wells, but it is used in this exercise to allow a finite probability of very rapid flow and transport pathways through the fractured tuff. The attachment and detachment rate distributions (Table 6, Group 3) are correlated with the retardation factor probabilities in Group 3 of Table 6.

Figure 6 shows the cumulative distributions of Da_{att} , Da_{det} , and $Da_{att}+Da_{det}$ resulting from a 5000 realization GoldSim calculation. The sum of the two Damkohler numbers drops below 100 in less than 5 percent of the realizations and below 10 in less than 1 percent of the realizations. In these few cases, the assumption of local equilibrium may not be valid. However, for those cases,

the residence times are very small due to very low porosity and high specific discharge. Specifically, for the simulations in which $Da_{att} + Da_{det} < 100$, travel times through the tuff aquifer estimated from these parameters are less than 20 years, which is much less than the presumed regulatory time frame of 10,000 years. Therefore, a slight overestimate of travel time as a result of assuming local equilibrium for these few cases should not have an impact on PA results. Also, it should be noted that the largest filtration rate constant observed in the C-wells field tests (0.2 hr^{-1}) was associated with the shortest travel time in any of the tests. Although it is not possible to establish a correlation between filtration rates and travel times from this single observation, if an inverse correlation exists, then the above analysis would be conservative.

In about 30 percent of the realizations Da_{det} is less than 10, indicating that its contribution may not be modeled well with the equilibrium approximation. However, in such cases, using an equilibrium approximation leads to errors on the side of conservatism with this term because retention of colloids on the fracture surfaces is underestimated. The attachment terms, as shown in Figure 6, are always greater than 10. If there is any error in the attachment term (for those less than 100), the equilibrium approximation is not conservative, but as stated above, the errors can only lead to overestimating retardation by about 20 years, which is an error that will have no consequence in the PA calculations (Recall also that Bahr and Rubin (1987) caution that both Damkohler numbers, $Da_{att} + Da_{det}$, should be used to assess the kinetic term).

Finally, a particularly conservative aspect of this analysis is that there is no probability of a zero detachment rate constant. In reality, it is very likely that some colloids will irreversibly attach. Although only a small fraction of the injected microspheres were recovered in the C-wells tracer tests (Figures 1 and 2), the retardation factors derived from the kinetic parameters that were used to fit the data will lead to predictions of 100% recovery.



DTN: SN0004T0571599.004 (for flow rates). Output Data -- DTN LA0004AW12213S.001.

Figure 6. Damkohler Number Distributions for Attachment and Detachment Kinetic Rates (Table 6) for Fractured Tuff

6.1.5 Uncertainty in Assumptions

Appropriate caution should be exercised when using the probability density functions of Figures 3 through 5 to represent the behavior of radionuclide-bearing colloids in fractured volcanic tuffs. One reason for this caution is that it is not known how well the polystyrene microspheres represent such colloids. Although they were chosen for their similarity in size, surface charge, and hydrophilicity to colloids that may facilitate radionuclide transport, the microspheres certainly differ from such colloids in their surface chemistry, shape, and density. The density of the microspheres is 1.055 g/cm^3 (almost neutrally buoyant), as compared to natural or waste-form colloids, which should have a density of $2.0\text{-}2.5 \text{ g/cm}^3$. It can be shown that the latex spheres should settle (by gravity) at about the same rate as a 2.5 g/cm^3 colloid that is ~ 5.2 times smaller in diameter (see last term of Equation 6 in Section 6.2.2). Waste-form colloids are about 120-160 nm in diameter (DTN: LL991109751021.094), so the microspheres used in the C-wells tests (ranging from 280- to 640-nm diameter) should have actually settled more slowly than waste-form colloids, which is conservative. The larger microspheres would also have diffused more slowly than waste-form colloids (diffusivity is inversely proportional to diameter), which is conservative. However, the microspheres would have been more prone to inertial collisions with fracture surfaces than waste-form colloids (interception is proportional to diameter squared), which is nonconservative.

Another reason for exercising caution in using the probability density functions of Figures 3 through 5 is that all C-wells observations were made over only a ~30-meter travel distance and for less than one year. Extrapolation to longer distances and time scales is an exercise in uncertainty. The flow conditions in the field tests were, by necessity, perturbed from natural flow conditions with significant forced gradients being imposed to induce tracer movement. Also, there were three significant flow interruptions during the Prow Pass Tuff test, of which at least the first two appeared to result in brief, large jumps in the colloid concentrations upon resumption of flow at approximately 1000 and 1250 hrs (see Figure 2). These spikes in colloid concentration were ignored when estimating colloid transport parameters. The retardation factor distribution generated in this analysis is based on the assumption that the Bullfrog Tuff and the Prow Pass Tuff are equally probable formation types through which colloids would travel in the saturated zone (Table 2). If the Prow Pass Tuff parameters were not considered due to the higher permeability in the Bullfrog Tuff (based on an argument suggesting that pathways through the saturated tuff are more likely in higher permeability units), then the resulting retardation factor distribution would show higher probabilities for lower values. The net result of dropping the Prow Pass data would be to double the probabilities of the smaller retardation factors and the larger detachment rate constants.

6.1.6 Model Summary: Fractured Tuff Colloid Retardation Factors

At the field scale, colloid retardation factors in fractured tuff can be estimated as attachment rates of colloids to fracture walls divided by detachment rates of colloids from fracture walls. The transport model, RTA V1.1, is parameterized such that it is used to estimate these attachment and detachment rate parameters by matching model predictions to the microsphere transport data from the Bullfrog and Prow Pass tuff tracer tests at the C-wells complex. Since multiple tests were conducted, each providing different parameters, a distribution of retardation factors is developed to represent all of the different testing conditions and flow intervals tested. This distribution of retardation factors is used in predictive models that may be used in PA calculations.

6.1.7 Model Validation Summary: Fractured Tuff Colloid Transport

The kinetic model of colloid attachment and detachment in fractured tuffs (Equations 1 and 2) is validated by matching the field observations of microsphere transport at the C-wells (Figures 1 and 2). However, the use of the derived probability distribution of retardation factors in field-scale predictions requires that the local equilibrium approximation be valid. Therefore, an additional analysis (Section 6.1.4) evaluates the validity of the equilibrium approximation at the field scale and demonstrates that it is either accurate or conservative.

6.2 COLLOID TRANSPORT IN ALLUVIAL MATERIAL

6.2.1 Background

Retardation factors for colloids, natural or synthetic, have not been measured in the alluvial aquifer downgradient of Yucca Mountain. There is a good possibility that such parameters will be measured within the next few years if the currently planned alluvial tracer testing is implemented. However, TSPA requires estimates of retardation factors for colloids in alluvium now. Therefore, this portion of the AMR provides a theoretical approach based, in part, on field tests at other alluvial aquifers. Those alluvial aquifers considered are a sand aquifer at the Canadian Forces Base, Borden, Ontario, studied by Bales et al. (1997) and a sand aquifer on Cape Cod, Massachusetts, studied by Harvey and Garabedian (1991). Direct comparison between these aquifers and the valley fill alluvium in the Yucca Mountain flow system is impossible because the Yucca Mountain alluvium has not been characterized to date. However, alluvial material in Yucca Flat, which is less than 50 miles from Yucca Mountain, is characterized mostly by sand with finer material, including clay and silt, accounting for less than 25 percent of the weight fraction in the samples analyzed by Bechtel (1998b). Compared with the clean, well-sorted sands of the other study sites, it is likely that the Yucca Mountain alluvium, like the Yucca Flat alluvium, is less well-sorted and that the range of grain sizes is larger. Further, the interstitial pore spaces between larger grains, rocks, and cobbles are likely to be filled with smaller grain sands and silts. Still, the theoretical approach taken here accounts for variable grain sizes. Therefore, because the Yucca Mountain alluvium, like the other two sites where colloid transport was studied, is characterized by flow-through porous media (as opposed to fractured tuff), the approach taken by Harvey and Garabedian (1991) is the best approach, considering the absence of Yucca Mountain specific data. The approach allows specifically for the grain size distribution to be specified. Thus, the method tested with site colloid transport data at Cape Cod is extended, incorporating estimates of the grain sizes specific to the Yucca Mountain system.

6.2.2 Parameters for Calculation of Retardation Factors

The retardation factor, R , by definition implies equilibrium conditions. Thus, the rate of accumulation of colloids in the attached phase is zero and R , for colloid transport in alluvial material, is approximated, similarly as in Equation 3, as follows:

$$R = 1 + \frac{\rho_a k_f}{\theta k_r} \quad (\text{Eq. 4})$$

where

ρ_a denotes the density of the alluvial material

θ is the porosity

k_f is the rate of colloid attachment onto the immobile material

k_r is the detachment rate.

Equation 4 is directly derived from Harvey and Garabedian (1991, Equation 1 and Equation 5) or Bales et al. (1997, Equation 3). Colloid attachment, k_f , is estimated with colloid filtration theory, which considers the diameter of the porous media grains, the size of the colloids, the single-collector efficiency (the rate at which colloids strike a porous media grain divided by the rate at which colloids move toward the grain), and the collision efficiency factor (the efficiency with which collisions between colloids and immobile grains results in immobilization of the colloid). The standard colloid filtration theory equation for the rate of attachment is given by Harvey and Garabedian (1991, Equation 2) as:

$$k_f = v \frac{3(1-\theta)}{2d} \alpha \eta, \quad (\text{Eq. 5})$$

where

v is the fluid velocity
 d is the diameter of the porous media grains
 α is the collision efficiency factor
 η is the single-collector efficiency.

η can be estimated by $\eta = \eta_D + \eta_I + \eta_G =$:

$$0.9 \left[\frac{kT}{\mu d_p dv} \right]^{2/3} + 1.5(d_p/d)^2 + \frac{(\rho_p - \rho)gd_p^2}{18\mu v}. \quad (\text{Eq. 6})$$

where

η_D is the colloid collector collision caused by Brownian motion
 η_I is the colloid collector collision caused by interception
 η_G is the colloid collector collision caused by settling
 k is the Boltzmann constant
 T is the solute temperature
 μ is the fluid viscosity
 d_p is the colloid diameter
 d is the diameter of the porous media grains
 ρ is the fluid density
 ρ_p is the colloid density
 g is gravity.

The collision efficiency factor, α , is estimated from field experiments by Harvey and Garabedian (1991, Table II) and ranges between 0.005 (bacterial colloids) and 0.025 (microsphere colloids). The collision efficiency factor represents the number of colloid-collector collisions that occur before attachment (e.g., a value of 0.005 indicates that 500 collisions occur before attachment). Whereas, very small values represent unfavorable conditions for filtration, larger values indicate

favorable conditions (when $\alpha=1$, filtration occurs with every collision, and colloids are least mobile).

If all of the parameters in Equations 5 and 6 were well known and non-varying, then computing k_f would be trivial. However, there is uncertainty in the grain size, the colloid size, the alluvium porosity, the specific discharge (flux), and the collision efficiency factor. Therefore, those terms are considered with distributions spanning their range of uncertainty and are reported in Table 7 (sources reported in Section 4). The terms in Equations 5 and 6 that are held constant are k , T , μ , ρ , ρ_p , and g . T , as reported in Section 4, is held constant at 25 degrees Celsius (DTN: GS950408318523.001), thus removing and temperature dependent variability in other parameters in this analysis.

In addition to k_f , the calculation of a retardation factor in Equation 4 requires k_r . However, filtration theory does not provide a method for estimating detachment of colloids from grains with such measurable parameters as particle size, grain size, or fluid velocity. Therefore, the detachment rate is also treated as an uncertain parameter. The range for the distribution of k_r is estimated from reported field experiments of colloid transport in the Borden aquifer (Bales et al. 1997, Table 3, p. 645) and from the detachment rates of colloids from fractured tuff at Yucca Mountain (Section 6.1 of this report). The range of detachment rates used in this analysis spans nearly six orders of magnitude. This range represents our uncertainty due to the lack of data for the system under consideration. It captures both ends of the spectrum for what are considered to be plausible or possible values for the saturated alluvium downgradient of Yucca Mountain.

Table 7. Parameters for Retardation Factor Calculations and Uncertainty Range Distributions

Parameter	Min	Max	Distribution
Grain size (d) (cm) ⁽¹⁾	0.02	0.11	Uniform
Colloid Size (d_p) (cm)	6.0E-07	4.5E-05	Uniform
Alpha (α)	.005	.025	Uniform
Porosity (θ)	0 (min limit)	1 (max limit)	Truncated Normal (mean = 0.18, $\sigma=0.055$)
Flux (q) (m/yr) ⁽²⁾	0.2	20	Discrete (0.2,24%; 2.0,52%; 20.0,24%)
Detachment Rate (k_d) (1/hr)	1.0E-05	3.33	Log-Uniform

DTNs: SN0004T0571599.004 (for porosity), SN0004T0501600.004 (for flux), LL991109751021.094 (for colloid size). Other sources: Marshall et al. (1996) and Bechtel (1998a, 1998b) (for grain size), Harvey and Garabedian (1991) (for alpha), and Bales et al. (1997) and Table 6 of this report (for detachment rate).

NOTES: ⁽¹⁾ Additional ranges of grain sizes are considered in Section 6.2.5. Basis for this assumption discussed in Section 5.

⁽²⁾ The velocity (v) in Equations 5 and 6 is computed from the flux and porosity; $v=q/\theta$

6.2.3 Calculation of Retardation Factor Distribution

Using the parameter distributions in Table 7, a distribution of retardation factors for colloids in saturated alluvial material (Equations 4 through 6) is computed with GoldSim V6.03 (STN: 10296-6.03-00). Also, the groundwater temperature is set at 25 degrees Celsius in these simulations as described in Table 2 (DTN: GS950408318523.001). The model draws from the prescribed parameter distributions to compute a new retardation factor for each realization. Figure 7 shows the GoldSim schematic for computing retardation factors using Equations 4 through 6. Figure 8 shows the results from five different 10,000 realization simulations. Although each simulation shown in Figure 8 results from sampling independently the distributions for each uncertain parameter listed in Table 7, all five simulations are virtually identical as a result of 10,000 realizations in each simulation. The curve in Figure 8 provides a basis from which PA can create a discrete probability distribution of retardation factors for their simulations.

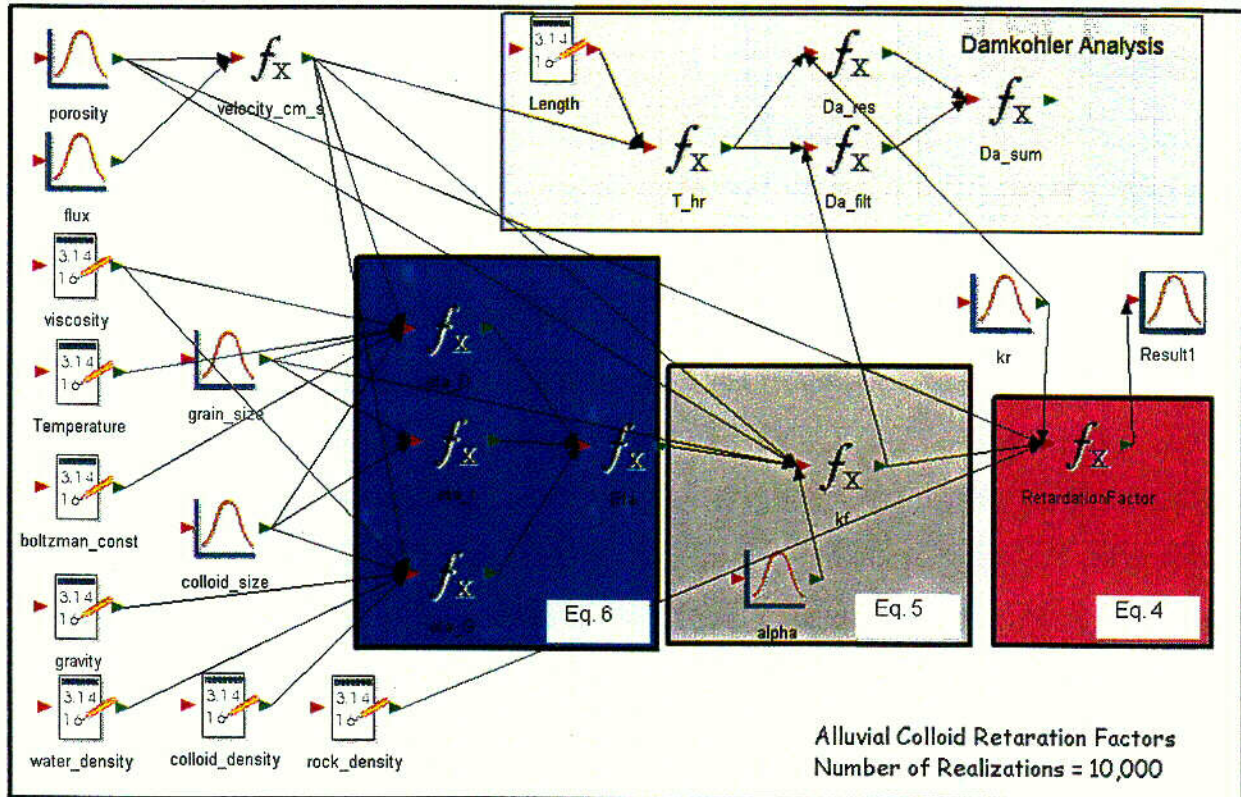
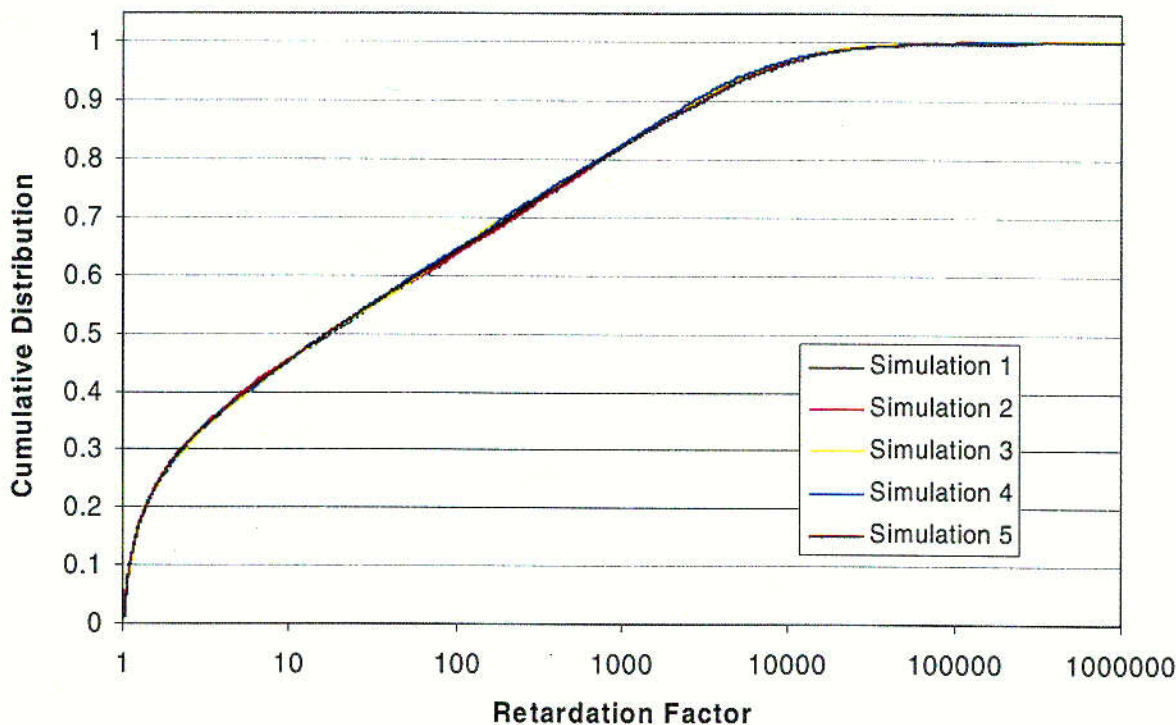


Figure 7. Schematic of GoldSim Model of Equations 4-6 for Alluvial Colloid Retardation Factors

C-1



DTNs: SN0004T0571599.004 (for porosity), SN0004T0501600.004 (for flux), LL991109751021.094 (for colloid size). Other sources: Marshall et al. (1996) and Bechtel (1998a, 1998b) (for grain size), Harvey and Garabedian (1991) (for alpha), and Bales et al. (1997) and Table 6 of this report (for detachment rate). Output Data – DTN LA0004AW12213S.001.

NOTES: Results of all five simulations are essentially superimposed.

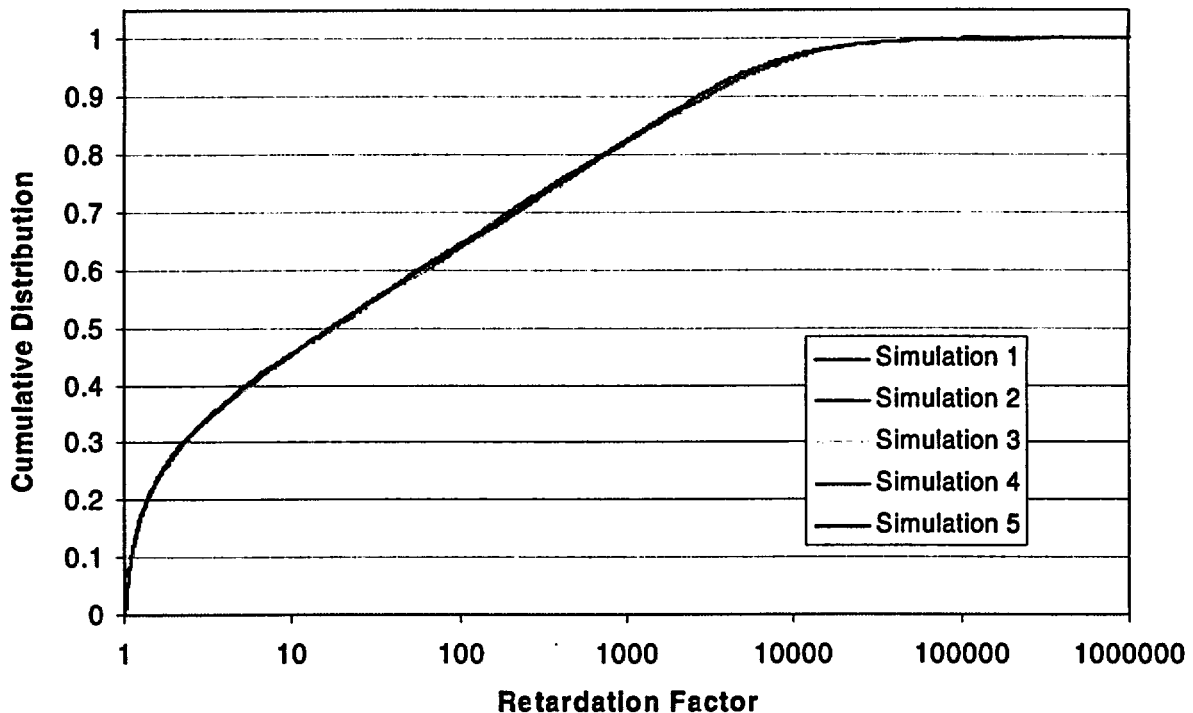
Figure 8. Retardation Factor Distribution For Five Simulations

6.2.4 Validity of the Local Equilibrium Assumption in Estimating Retardation for Saturated Alluvium

Whereas high porewater velocities in the fractured tuff brings the assumption of local equilibrium for colloid retardation into question, there appears to be no such issue in the alluvial aquifer. The Damkohler numbers for the alluvial system, as shown in Figure 7, are computed using a length scale of 5000 meters. Due to the high porosity, $Da_{att} + Da_{det}$ is always greater than 1000 for the distributions of specific discharge (flux) and porosity in the alluvium, discussed earlier in this section. Figure 9 shows the Damkohler number distributions (computed with GoldSim V6.03 (STN: 10296-6.03-00) as shown in Figure 7) associated with the estimation of retardation factors computed for Figure 8. Although Da_{att} never drops below 100, Da_{det} drops below 100 in about 10 percent of the realizations. For these cases, estimating retardation factors with the local equilibrium assumption leads only to conservative errors as retention on the immobile surfaces would be larger if modeled with a kinetic formulation.

As mentioned in Section 6.1.4, the use of retardation factors is conservative because there is no probability of a zero detachment constant. In reality, it is very likely that some colloids will irreversibly attach to immobile surfaces.

C-2



DTNs: SN0004T0571599.004 (for porosity), SN0004T0501600.004 (for flux), LL991109751021.094 (for colloid size). Other sources: Marshall et al. (1996) and Bechtel (1998a, 1998b) (for grain size), Harvey and Garabedian (1991) (for alpha), and Bales et al. (1997) and Table 6 of this report (for detachment rate). Output Data – DTN LA0004AW12213S.001.

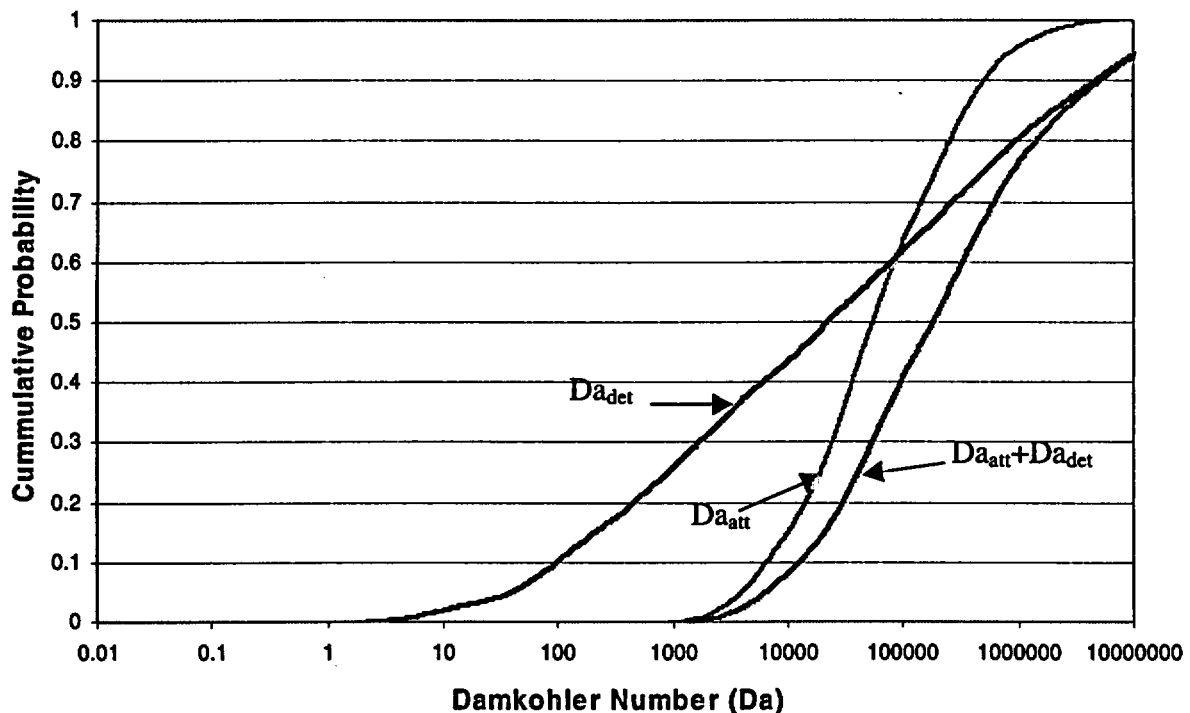
NOTES: Results of all five simulations are essentially superimposed.

Figure 8. Retardation Factor Distribution For Five Simulations

6.2.4 Validity of the Local Equilibrium Assumption in Estimating Retardation for Saturated Alluvium

Whereas high porewater velocities in the fractured tuff brings the assumption of local equilibrium for colloid retardation into question, there appears to be no such issue in the alluvial aquifer. The Damkohler numbers for the alluvial system, as shown in Figure 7, are computed using a length scale of 5000 meters. Due to the high porosity, $Da_{att} + Da_{det}$ is always greater than 1000 for the distributions of specific discharge (flux) and porosity in the alluvium, discussed earlier in this section. Figure 9 shows the Damkohler number distributions (computed with GoldSim V6.03 (STN: 10296-6.03-00) as shown in Figure 7) associated with the estimation of retardation factors computed for Figure 8. Although Da_{att} never drops below 100, Da_{det} drops below 100 in about 10 percent of the realizations. For these cases, estimating retardation factors with the local equilibrium assumption leads only to conservative errors as retention on the immobile surfaces would be larger if modeled with a kinetic formulation.

As mentioned in Section 6.1.4, the use of retardation factors is conservative because there is no probability of a zero detachment constant. In reality, it is very likely that some colloids will irreversibly attach to immobile surfaces.



DTNs: SN0004T0571599.004 (for porosity), SN0004T0501600.004 (for flux), LL991109751021.094 (for colloid size). Other sources: Marshall et al. (1996) and Bechtel (1998a, 1998b) (for grain size), Harvey and Garabedian (1991) (for alpha), and Bales et al. (1997) and Table 6 of this report (for detachment rate). Output Data – DTN LA0004AW12213S.001.

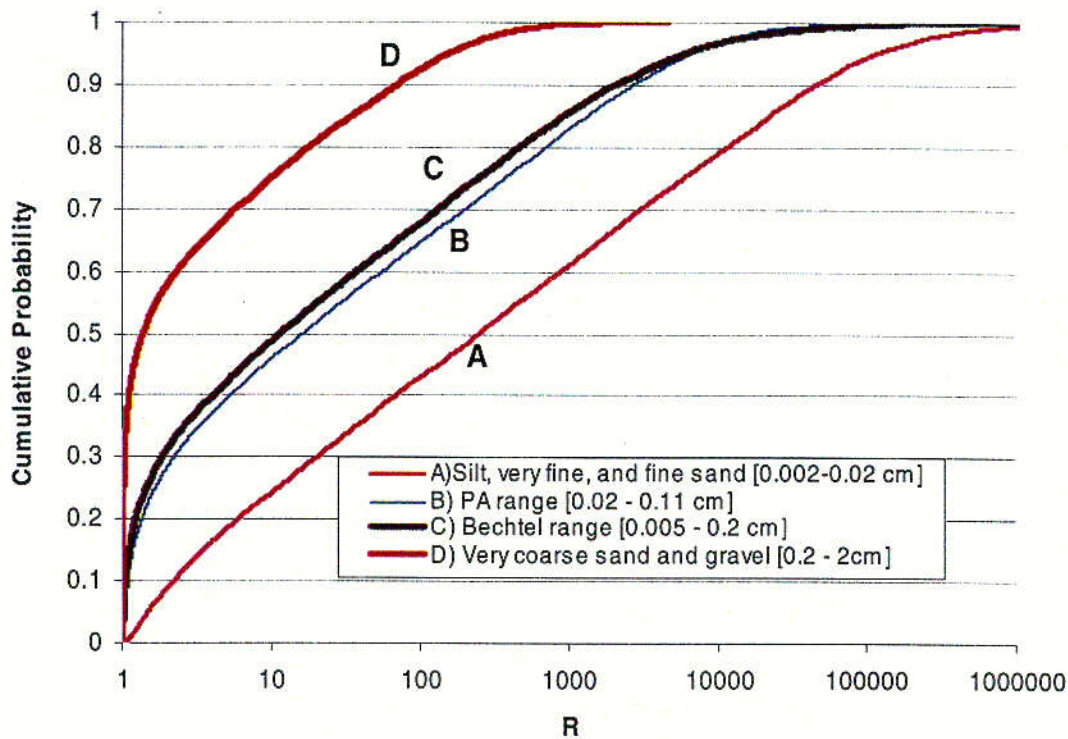
Figure 9. Damkohler Number Distributions for Attachment and Detachment Kinetic Rates (Table 6) for Alluvium

6.2.5 Uncertainty in Assumptions

Although the GoldSim V6.03 (STN: 10296-6.03-00) simulation shown in Figure 8 captures ranges of uncertainty in the parameter distributions leading to the computation of alluvial retardation factors, there is still uncertainty in the ranges and shapes of those distributions due to the paucity of data for the alluvial system. One of the most important parameter distributions affecting the shape of the simulated retardation factor distribution is the grain size distribution. For the purposes of this AMR, a mixture of fine, medium, and course sand has been assumed to be representative of the alluvial material (Table 2). However, if the valley fill deposits are actually coarser or finer, then the retardation factor distribution will be shifted. Although the valley fill deposits of the system under consideration are only now being characterized and have not been documented in a referenceable format for this AMR, there is the possibility that the material may be poorly sorted and that the interstices between pebbles and cobbles will be filled with fine-grained material. Under such conditions, the fine-grained material surface area may increase the collector efficiency. Similarly, without more detailed understanding of the system under consideration, there is some possibility that the valley fill material may actually be characterized by only coarser material, particularly in prominent flow pathways and subsurface channels. Therefore, Figure 10 compares the simulated retardation factor distribution for four different grain size distributions: (a) a range representing fine grain material, between 0.002 and 0.02 cm ; (b) the range considered in Figure 8, between 0.02 cm and 0.11 cm; (c) the range for

sand reported by Bechtel (1998b), which is between 0.005 and 0.2 cm; and (d) a range representing very coarse grains ranging only from 0.2 cm and 2.0 cm. Clearly, the distribution of retardation factors is sensitive to the grain-size distribution. Yet, the range for all cases is still large, spanning between 5 and 7 orders of magnitude, thus indicating significant uncertainty in the process due to the lack of site-specific data. The range used in Figure 8 and the range from Bechtel (1998b) lead to very similar distributions, with the Bechtel range providing slightly smaller retardation factors due to the coarser grains. However, a detailed distribution accounting for exact percentages of each subrange in the grain-size distribution, including the silts and clays, might actually lead to increases in R . Such an analysis is only warranted once the Yucca Mountain alluvium grain-size distributions have been documented.

One must remember that this is strictly a theoretical assessment of the colloid filtration process. Reduction in uncertainty will require detailed measurements of actual colloid transport process in the alluvial material of interest with field and laboratory experiments coupled with additional sensitivity analyses. Although case (b) described above may be plausible, it is conservative in the absence of site-specific data to assume (Table 2) the grain-size distribution of case (a) because it leads to lower retardation factors than case (b). Another parameter that needs to be better assessed for this system is the collosion efficiency factor, α . Although it has much less impact on the resulting retardation factor distribution, its range is acquired strictly from other systems in the current analysis.



DTNs: SN0004T0571599.004 (for porosity), SN0004T0501600.004 (for flux), LL991109751021.094 (for colloid size). Other sources: Marshall et al. (1996) and Bechtel (1998a, 1998b) (for grain size), Harvey and Garabedian (1991) (for alpha), and Bales et al. (1997) and Table 6 of this report (for detachment rate). Output Data – DTN LA0004AW12213S.001.

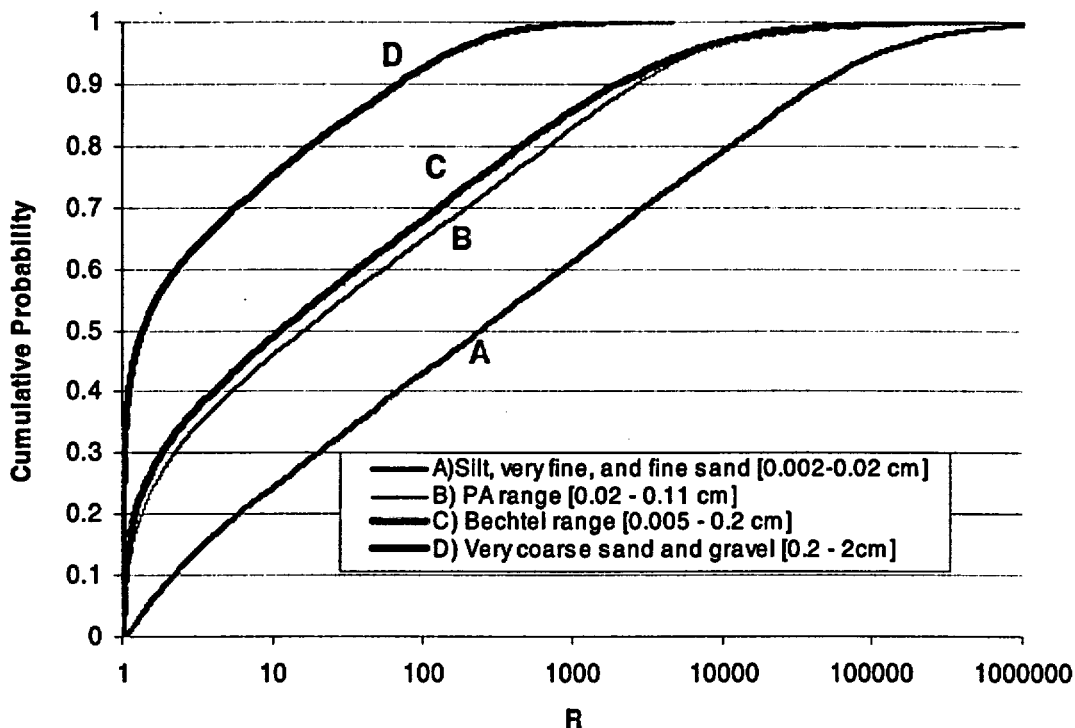
NOTES: PA range is the original distribution of retardation factors developed in this study and used by Performance Assessment. Bechtel range is the grain-size range for sand reported by Bechtel (1998b). For the extremely coarse grains, D, Equations 5-6 may not be appropriate and, hence, Equation 4 may not properly represent colloid retardation due to attachment for this extreme size of grains. However, there is no evidence to suggest that such coarse grains are representative of the Yucca Mountain alluvium.

Figure 10. Comparing GoldSim Simulations of Retardation Factors for Four Different Grain-Size Diameter Distributions

6.2.6 Conceptual Model Summary: Alluvial Colloid Retardation Factors

Conceptually, this model links attachment rates and detachment rates of colloids together to yield a colloid retardation factor in alluvium. For large enough time and space scales, the ratio of attachment rates to detachment rates added to one yields an equilibrium retardation factor that approximates the processes that inhibit migration of colloids in alluvial material. This model bases the attachment rates on classic colloid filtration theory, which predicts the attachment rate using such measurable quantities as colloid size, grain size, water flux, colloid density, etc. (Equation 6). Because all of these quantities are variable, the distribution of attachment rates is

C-3



DTNs: SN0004T0571599.004 (for porosity), SN0004T0501600.004 (for flux), LL991109751021.094 (for colloid size). Other sources: Marshall et al. (1996) and Bechtel (1998a, 1998b) (for grain size), Harvey and Garabedian (1991) (for alpha), and Bales et al. (1997) and Table 6 of this report (for detachment rate). Output Data – DTN LA0004AW12213S.001.

NOTES: PA range is the original distribution of retardation factors developed in this study and used by Performance Assessment. Bechtel range is the grain-size range for sand reported by Bechtel (1998b). For the extremely coarse grains, D, Equations 5-6 may not be appropriate and, hence, Equation 4 may not properly represent colloid retardation due to attachment for this extreme size of grains. However, there is no evidence to suggest that such coarse grains are representative of the Yucca Mountain alluvium.

Figure 10. Comparing GoldSim Simulations of Retardation Factors for Four Different Grain-Size Diameter Distributions

6.2.6 Conceptual Model Summary: Alluvial Colloid Retardation Factors

Conceptually, this model links attachment rates and detachment rates of colloids together to yield a colloid retardation factor in alluvium. For large enough time and space scales, the ratio of attachment rates to detachment rates added to one yields an equilibrium retardation factor that approximates the processes that inhibit migration of colloids in alluvial material. This model bases the attachment rates on classic colloid filtration theory, which predicts the attachment rate using such measurable quantities as colloid size, grain size, water flux, colloid density, etc. (Equation 6). Because all of these quantities are variable, the distribution of attachment rates is

created by drawing on distributions of all the quantities. Similarly, the detachment rate is represented with a distribution rather than a fixed value. Finally, the retardation factor distribution is computed by drawing from the distribution of attachment and detachment rates.

6.2.7 Model Summary: Alluvial Colloid Retardation Factors

The model in this portion of the AMR represents the processes associated with retardation factors for alluvial colloid transport to be used in other analyses such as Yucca Mountain PA. The model represents the retardation factor as a function of attachment rate of colloids *to* and detachment rate of colloids *from* immobile grains. The attachment rates are estimated with classic colloid filtration theory. Such theory does not provide for evaluation of detachment rates. Therefore, detachment rates are approximated based on detachment rates from fracture surfaces (this AMR) and from field observations in a sand aquifer at another location (Bales et al. 1997). Attachment rates are uncertain due to the range of uncertainty in the input parameters used in the model. Therefore, a distribution of attachment rates is developed via Monte Carlo simulation, which samples the ranges of uncertainty in all parameters. Similarly, observed detachment rates are uncertain. The model linking attachment rates and detachment rates to retardation factors draws from the distributions of attachment and detachment rates and produces a distribution of retardation factors. This distribution, then, represents the range in uncertainty of alluvial colloid retardation factors. It is in a form such that PA calculations can draw from it to capture the uncertainty in alluvial colloid retardation factors.

6.2.8 Model Validation Summary: Alluvial Colloid Transport

The development of retardation factors for alluvial colloid transport in this AMR is classified as a model because a set of equations are used to represent the physical and chemical phenomena associated with such retardation. It is not a predictive process model in that it is not used in this AMR to predict travel times and concentrations of colloids or radionuclides. Rather, it is a model specifically for estimating a transport parameter based on system properties. This model cannot currently be validated against Yucca Mountain laboratory or field observations because those data have not yet been collected and analyzed. However, the equations used and, hence, the model by definition have been validated through technical review and publication in the open literature. Specifically, the equations used to estimate colloid filtration (Equations 5 and 6) are well established in the literature. Harvey and Garabedian (1991) used the theory in a field demonstration of colloid transport in a sand aquifer, demonstrating the appropriateness of the equations. Those equations are adopted in this analysis and utilized. The primary differences between the analysis of Harvey and Garabedian (1991) and this AMR are: (1) The input parameters are site specific (Equation 6); that is, the groundwater flux, grain sizes, colloid sizes, etc., are unique to the system under consideration. (2) We assume equilibrium conditions, which is a necessary condition for Yucca Mountain PA models. Thus, there is no accumulation of attached colloids due to irreversible (or very slow) kinetics. This assumption is tested and evaluated in Section 6.2.4 of this AMR and demonstrated to be either accurate or conservative. Until the appropriate data are collected and analyzed for the Yucca Mountain system, this model represents the best use of established, published theory for estimating retardation factors for colloids in alluvium.

7. CONCLUSIONS

This AMR addresses the retardation mechanisms associated with the transport of colloids in the fractured tuff and alluvial systems of the Yucca Mountain saturated zone. In the fractured tuff, tracer experiments under forced gradient conditions have utilized synthetic microspheres as analogs of contaminant-bearing colloids. Analysis of the breakthrough curves of these microspheres provides estimates of the ranges of retardation factors that may be associated with colloid migration over much larger distances and time scales than were sampled during the tracer tests. In this analysis, the kinetic attachment and detachment rates estimated for the microsphere tracer tests are abstracted into a single retardation factor. The validity of this abstraction is demonstrated by showing that (1) colloid transport predictions using the retardation factor and the full kinetic attachment and detachment rate expressions do not differ over almost the entire range of travel times expected for the fractured tuffs, and (2) the retardation factor provides conservative predictions for very short travel times when the kinetic and equilibrium predictions differ.

Whereas field and laboratory studies of colloid and/or microsphere transport have been conducted for saturated fractured tuff, there are currently no similar studies that have been performed for the saturated alluvial system. Therefore, in this AMR, a theoretical model is employed to estimate the attachment of colloids onto immobile alluvial material. The model uses a well-established methodology that has been applied to colloid transport in other saturated porous media systems. The theory, however, does not supply a method for estimating the detachment of colloids from immobile porous media. Therefore, rates estimated for detachment from fractures as well as detachment rates estimated in another instrumented aquifer are used. The resulting estimated retardation factor distribution spans over six orders of magnitude, thus capturing both ends of the spectrum of possible retardation factors for the currently untested system.

The PA method for computing saturated-zone colloid transport requires an equilibrium-based retardation factor. For both the fractured tuff and alluvial aquifer, the retardation factors have been estimated from kinetic rates of attachment and detachment of colloids onto immobile surfaces. However, this local equilibrium assumption may not be accurate when residence times are small relative to the rates of attachment and detachment of colloids from immobile surfaces. A simple Damkohler analysis shows that assuming local equilibrium is generally suitable for both the fractured tuff and the alluvial aquifer. There are a few cases in the fractured tuff when assuming local equilibrium leads to overestimates of the attachment rate of colloids to fracture surfaces, which, in turn, leads to nonconservative overestimation of retardation. However, for those cases, the retardation factors and the residence times are so small that the overestimation results, at most, in tens of years additional residence of colloids in the fracture tuff, which is an insignificant time period relative to the time scales impacting PA.

Although this analysis represents a reasonable approach for estimating field-scale retardation factors for colloid transport, there are inherent uncertainties that should be considered when evaluating the confidence in results obtained with these parameters. For fractured tuff, this analysis used extensive field data. However, the data were collected under stressed conditions that differ from those associated with the ambient system. Namely, transport of colloids was

measured under conditions involving forced groundwater gradients induced by well pumping. Further, the spatial scale of the field-scale experiment is only about 100 meters, and the measurements were conducted over a time period less than 1 year. The differences between the test scales and those considered for the entire system should always be considered when evaluating model confidence. Whereas an extensive set of field experiments were conducted for colloid transport in fractured tuff, such experiments have not yet been conducted for alluvial material. Therefore, determination of colloid retardation factors for alluvial material was dependent on an established theoretical model but estimated site-specific properties. The uncertainty in property parameters was accounted for with distributions which were then sampled in a Monte Carlo fashion for the calculation of a retardation factor distribution. The range associated with the resulting retardation factor distribution spans six orders of magnitude, indicating the uncertainty associated with site-specific retardation factors for Yucca Mountain alluvium. Although the shape of the distribution curve changes, depending on assumptions about input parameter ranges, the large range in the resulting distribution clearly identifies the uncertainty. However, the PA use of this distribution is appropriate. By sampling the entire distribution, PA calculations will yield a large range of results, thereby indicating the uncertainty with the alluvial retardation parameter.

The data and model developed by this analysis are included in DTNs: LA0004AW12213S.001, LA0002PR831231.003, and LA9912PR831231.006.

This document may be affected by technical product input information that requires confirmation. Any changes to the document that may occur as a result of completing the confirmation activities will be reflected in subsequent revisions. The status of the input information quality may be confirmed by review of the Document Input Reference System database.

8. INPUTS AND REFERENCES

8.1 DOCUMENTS CITED

- Bahr, J.M. and Rubin, J. 1987. "Direct Comparison of Kinetic and Local Equilibrium Formulations for Solute Transport Affected by Surface Reactions." *Water Resources Research*, 23, (3), 438-452. Washington, D.C.: American Geophysical Union. TIC: 246894.
- Bales, R.C.; Li, S.; Yeh, T.-C.J.; Lenczewski, M.E.; and Gerba, C.P. 1997. "Bacteriophage and Microsphere Transport in Saturated Porous Media: Forced-Gradient Experiment at Bordon, Ontario." *Water Resources Research*, 33, (4), 639-648. Washington, D.C.: American Geophysical Union. TIC: 246892.
- Bechtel Nevada 1998a. *Hydrogeologic Characterization of the Unsaturated Zone at the Area 3 Radioactive Waste Management Site: Volume 1 - Data Interpretations*. DOE/NV/11718-204. Las Vegas, Nevada: Bechtel, Nevada. On Order Library Tracking Number-247707
- Bechtel Nevada 1998b. *Hydrogeologic Characterization of U-3 at Collapse Zone: Data Report*. DOE/NV/11718-199. Las Vegas, Nevada: Bechtel, Nevada. On Order Library Tracking Number-247705
- CRWMS M&O 1999a. *Abstraction of Colloid-Facilitated Pu Transport Modeling, Rev. 01. ID: B2005; Activity: SPP1075*. Work Direction and Planning Document. Las Vegas, Nevada: CRWMS M&O. ACC: MOL.19990707.0110.
- CRWMS M&O 1999b. *Conduct of Performance Assessment*. Activity Evaluation, September 30, 1999. Las Vegas, Nevada: CRWMS M&O. ACC: MOL.19991028.0092.
- CRWMS M&O 2000a. *Colloid-Associated Radionuclide Concentration Limits: ANL ANL-EBS-MD-000020 REV 00*. Las Vegas, Nevada: CRWMS M&O. ACC: MOL.20000329.1187.
- CRWMS M&O 2000b. *Uncertainty Distribution for Stochastic Parameters*. ANL-NBS-MD-000011 REV 00. Las Vegas, Nevada: CRWMS M&O. Submit to RPC URN-0189
- DOE (U.S. Department of Energy) 2000. *Quality Assurance Requirements and Description*. DOE/RW-0333P, Rev. 10. Washington, D.C.: U.S. Department of Energy, Office of Civilian Radioactive Waste Management. ACC: MOL.20000427.0422.
- Dyer, J.R. 1999. "Revised Interim Guidance Pending Issuance of New U.S. Nuclear Regulatory Commission (NRC) Regulations (Revision 01, July 22, 1999), for Yucca Mountain, Nevada." Letter from Dr. J.R. Dyer (DOE/YMSCO) to Dr. D.R. Wilkins (CRWMS M&O), September 3, 1999, OL&RC:SB-1714, with enclosure, "Interim Guidance Pending Issuance of New NRC Regulations for Yucca Mountain (Revision 01)." ACC: MOL.19990910.0079.
- Harvey, R.W. and Garabedian, S.P. 1991. "Use of Colloid Filtration Theory in Modeling Movement of Bacteria through a Contaminated Sandy Aquifer ." *Environmental Science and*

Technology, 25, 178-185. Washington, D.C.: American Chemical Society. TIC: 245733.

Marshall, T.J.; Holmes, J.W.; and Rose, C.W. 1996. *Soil Physics*. 3rd Edition. Pages 207-212. New York, New York: Cambridge University Press. TIC: 246638.

Reimus, P.W. 1995. *The Use of Synthetic Colloids in Tracer Transport Experiments in Saturated Rock Fractures*. Ph.D. dissertation. LA-13004-T. Los Alamos, New Mexico: Los Alamos National Laboratory. TIC: 240694.

Reimus, P.W.; Adams, A.; Haga, M.J.; Humphrey, A.; Callahan, T.; Anghel, I.; and Counce, D. 1999. *Results and Interpretation of Hydraulic and Tracer Testing in the Prow Pass Tuff at the C-Holes*. Milestone SP32E7M4. Los Alamos, New Mexico: Los Alamos National Laboratory. TIC: 246377.

Valocchi, A.J. 1985. "Validity of the Local Equilibrium Assumption for Modeling Sorbing Solute Transport through Homogeneous Soils." *Water Resources Research*, 21, (6), 808-820. Washington, D.C.: American Geophysical Union. TIC: 223203.

8.2 CODES, STANDARDS, REGULATIONS, AND PROCEDURES

AP-3.10Q, Rev 2, ICN 0. *Analyses and Models*. Washington, D.C.: U.S. Department of Energy, Office of Civilian Radioactive Waste Management. ACC: MOL.200000217.0246.

AP-SL1Q, Rev. 2, ICN 4. *Software Management*. OCRWM Procedure. Washington, D.C.: U.S. Department of Energy, Office of Civilian Radioactive Waste Management. ACC: MOL.200000223.0508.

QAP-2-0, Rev. 5. *Conduct of Activities*. Las Vegas, Nevada: CRWMS M&O. ACC: MOL.19980826.0209.

8.3 SOFTWARE

Los Alamos National Laboratory. 1999. *Software Code: RTA V1.1*. V1.1. SUN. 10032-1.1-00.

Sandia National Laboratory. 2000. *Software Code: GoldSim V6.03*. V6.03. 10296-6.03-00.

8.4 SOURCE DATA, LISTED BY DATA TRACKING NUMBER

GS950408318523.001. Temperature, Thermal Conductivity, and Heat Flow Near Yucca Mountain, Nevada. Submittal date: 04/21/1995.

GS970708312314.007. Results of Hydraulic Conservative Tracer Tests in Miocene Tuffaceous Rocks at the C-Hole Complex, 1995 to 1997, Yucca Mountain, Nevada. Submittal date: 07/31/1997.

GS981008312314.002. Pump Test Data Collected at the C-Wells Complex 1/8/97 - 3/31/97.
Submittal date: 10/28/1998.

GS981008312314.003. Pumping Test Data Collected at the C-Well Complex, 5/7/96-12/31/96.
Submittal date: 10/28/1998.

GS990408312315.002. Transducer, Barometric Pressure, and Discharge Data Collected from
4/18/98 through 11/24/98 in Support of the Ongoing Hydraulic and Tracer Tests Being
Conducted at the UE-25 C-Well Complex, Nevada. Submittal date: 04/06/1999.

LA0002JC831341.001. Depth Intervals and Bulk Densities of Alluviums. Submittal date:
03/08/2000.

LA0002PR831231.001. Bullfrog Reactive Tracer Test Data. Submittal date: 02/04/2000.

LA9909PR831231.003. Interpretations of Bullfrog Reactive Tracer Test Data - Modeling Data.
Submittal date: 09/02/1999.

LA9909PR831231.005. Interpretations of Tracer Data - Modeling Data. Submittal date:
09/02/1999.

LAPR831231AQ99.001. Prow Pass Reactive Tracer Test Field Data. Submittal date:
02/10/1999.

LL991109751021.094. Data Associated with the Detection and Measurement of Colloids in
Scientific Notebook SN 1644. Submittal date: 01/10/2000.

SN0004T0501600.004. Updated Results of the Base Case Saturated Zone (SZ) Flow and
Transport Model. Submittal date: 04/10/2000. Submit to RPC URN-0292

SN0004T0571599.004. Uncertainty Distributions for Stochastic Parameters Revision to Include
New U Sorption Coefficients in the Alluvium and Supporting Electronic Files. Submittal date:
04/10/2000. Submit to RPC URN-0273